2017-09

Synthesizing graphene production with polymeric injection molding for enhancing EMI shielding effectiveness of plastics

Winstead, George K.

Monterey, California: Naval Postgraduate School

NAVAL POSTGRADUATE SCHOOL

MONTEREY, CALIFORNIA

THESIS

SYNTHESIZING GRAPHENE PRODUCTION WITH POLYMERIC INJECTION MOLDING FOR ENHANCING EMI SHIELDING EFFECTIVENESS OF PLASTICS

by

George K. Winstead

September 2017

Thesis Co-Advisors:	David C. Jenn Michael G. Pecht
Second Reader:	John M. Green

Approved for public release. Distribution is unlimited.

THIS PAGE INTENTIONALLY LEFT BLANK

REPORT DOCUMENTATION PAGE			*Form Approved OMB No. 0704–0188*

1. AGENCY USE ONLY *(Leave blank)*	**2. REPORT DATE** September 2017	**3. REPORT TYPE AND DATES COVERED** Master's thesis

4. TITLE AND SUBTITLE SYNTHESIZING GRAPHENE PRODUCTION WITH POLYMERIC INJECTION MOLDING FOR ENHANCING EMI SHIELDING EFFECTIVENESS OF PLASTICS	**5. FUNDING NUMBERS**
6. AUTHOR(S) George K. Winstead	
7. PERFORMING ORGANIZATION NAME(S) AND ADDRESS(ES) Naval Postgraduate School Monterey, CA 93943-5000	**8. PERFORMING ORGANIZATION REPORT NUMBER**
9. SPONSORING /MONITORING AGENCY NAME(S) AND ADDRESS(ES) N/A	**10. SPONSORING / MONITORING AGENCY REPORT NUMBER**

11. SUPPLEMENTARY NOTES The views expressed in this thesis are those of the author and do not reflect the official policy or position of the Department of Defense or the U.S. Government. IRB number ____N/A____.

12a. DISTRIBUTION / AVAILABILITY STATEMENT Approved for public release. Distribution is unlimited.	**12b. DISTRIBUTION CODE**

13. ABSTRACT (maximum 200 words)

Electromagnetic interference (EMI) shielding materials that are lighter in weight are critically needed for military applications. Existing materials utilized to suppress electromagnetic emissions involve homogenous metals or conductive fragments surrounded in polymeric material. The metal enclosures add significant weight and corrosion issues to the design, while the composite materials provide shielding effectiveness for only a limited range of frequencies. With the discovery of graphene, U.S. defense departments are quickly investing and investigating the applicability of graphene for EMI shielding. The research presented explores the production of graphene, development of an injection mold composite, and the shielding effectiveness of graphene for the range of frequencies stipulated in military standards. The study reveals that graphene, although highly conductive, rates poorly when shielding frequencies outlined in MIL-STD-461. However, in those discoveries, instances may still occur in which graphene may be deployed to assist in suppressing radiated emissions.

14. SUBJECT TERMS graphene, injection molding, polymeric, plastics, electromagnetic interference, EMI, shielding, product development	**15. NUMBER OF PAGES** 109
	16. PRICE CODE

17. SECURITY CLASSIFICATION OF REPORT	**18. SECURITY CLASSIFICATION OF THIS PAGE**	**19. SECURITY CLASSIFICATION OF ABSTRACT**	**20. LIMITATION OF ABSTRACT**
Unclassified	Unclassified	Unclassified	UU

NSN 7540–01-280-5500 Standard Form 298 (Rev. 2–89) Prescribed by ANSI Std. 239–18

THIS PAGE INTENTIONALLY LEFT BLANK

Approved for public release. Distribution is unlimited.

SYNTHESIZING GRAPHENE PRODUCTION WITH POLYMERIC INJECTION MOLDING FOR ENHANCING EMI SHIELDING EFFECTIVENESS OF PLASTICS

George K. Winstead
Civilian, Northrop Grumman Corporation
B.S., North Carolina State University, 1998
M.S., North Carolina State University, 2004

Submitted in partial fulfillment of the
requirements for the degree of

MASTER OF SCIENCE IN PRODUCT DEVELOPMENT

from the

NAVAL POSTGRADUATE SCHOOL
September 2017

Approved by: David C. Jenn
Thesis Co-Advisor

Michael G. Pecht
Thesis Co-Advisor, University of Maryland

John M. Green
Second Reader

Ronald Giachetti
Chair, Department of Systems Engineering

THIS PAGE INTENTIONALLY LEFT BLANK

ABSTRACT

Electromagnetic interference (EMI) shielding materials that are lighter in weight are critically needed for military applications. Existing materials utilized to suppress electromagnetic emissions involve homogenous metals or conductive fragments surrounded in polymeric material. The metal enclosures add significant weight and corrosion issues to the design, while the composite materials provide shielding effectiveness for only a limited range of frequencies. With the discovery of graphene, U.S. defense departments are quickly investing and investigating the applicability of graphene for EMI shielding. The research presented explores the production of graphene, development of an injection mold composite, and the shielding effectiveness of graphene for the range of frequencies stipulated in military standards. The study reveals that graphene, although highly conductive, rates poorly when shielding frequencies outlined in MIL-STD-461. However, in those discoveries, instances may still occur in which graphene may be deployed to assist in suppressing radiated emissions.

THIS PAGE INTENTIONALLY LEFT BLANK

TABLE OF CONTENTS

LIST OF FIGURES

LIST OF TABLES

LIST OF ACRONYMS AND ABBREVIATIONS

List of Acronyms

2D	two-dimensional
3D	three-dimensional
°C	Celsius
°F	Fahrenheit
A	amperes (*electricity)*
A	absorption loss
Å	angstrom
Ag	silver
AISI	American Iron and Steel Institute
Al	aluminum
AMC	Army Materiel Command (*United States*)
Ar	argon
atm	standard atmosphere (*unit of pressure*)
Au	gold
ave	average
B	correction factor for multiple reflections in thin shields
Be	beryllium
BTU	British thermal unit
c	speed of light constant
C	carbon (*chemistry*)
	Coulombs (*electricity*)
C	reflection loss constant, field type
CH_4	methane
cm	centimeters
Co	cobalt
CO_2	carbon dioxide
Cr	chromium
Cu	copper

CVD	chemical vapor deposition
d	electron sub-shell with a maximum of 10 electrons
dB	decibel
DOD	Department of Defense (United States)
e	elementary charge (charge of one electron)
E	electric field (*electricity*)
	Young's Modulus (*mechanical engineering*)
EMC	electromagnetic compatibility
EMI	electromagnetic interference
ESD	electrostatic discharge
et al.	et alii; (*latin*); and others
etc.	et cetera; (*latin*); and so forth
f	electron sub-shell with a maximum of 14 electrons
f	frequency
F	farad
Fe	iron
ft	foot/feet
g	gram
GPa	gigapascal
H	magnetic field (*electricity*)
	hydrogen (*chemistry*)
	Henry—the SI derived unit of electrical inductance
H_2	hydrogen gas
H_3PO_4	phosphoric acid
HCL	hydrochloric acid
HRC	Hardness Rockwell C
hr	hour/hours
H-SiC	hydrogen etched silicon carbide
i.e.	id est; (*latin*); in other words, for example
IMM	injection molding machine
j	imaginary unit

K	electron shell with principal quantum number, n=1
	Kelvin
l	liter
l	length of aperture for Eq. (20)
L	electron shell with principal quantum number, n=2
lpm	liters per minute
M	molar mass
	electron shell with principal quantum number, n=3
m	meter
m	exponential constant for Eq. (17)
mg	milligram
Mg	magnesium
MgO	magnesium oxide
$MgCl_2$	magnesium chloride
MIL-STD	military standard
min	minute
mL	milliliter
mm	millimeter
Mn	manganese
MPa	megapascal
n	exponential constant for Eq. (17)
	electron hybridization level
N	Newton (*unit of measure for force*)
	electron shell with principal quantum number, n=4
	nitrogen
Ni	nickel
nm	nanometer
O	oxygen
p	electron sub-shell with a maximum of six electrons
p_x	x-axis electron orbital in the p sub-shell
p_y	y-axis electron orbital in the p sub-shell
p_z	z-axis electron orbital in the p sub-shell

P	phosphorous
PDMS	polydimethylsiloxane
pg	page
pH	numeric scale used to specify the acidity of an aqueous solution
PMMA	polymethyl methacrylate
PVD	physical vapor deposition
QFD	quality function deployment
r	distance from EMI source to shield
R	reflection loss
R_0	ordinary Hall coefficient
R_1	extraordinary Hall coefficient
R_H	Hall coefficient
R_8	spontaneous Hall coefficient
RIE	reaction ion etch
rpm	revolutions per minute
RT	room temperature
s	seconds (*time*)
	electron sub-shell with a maximum of two electrons (*chemistry*)
	solid (*chemistry*)
S	Siemens (*electricity*)
	Sulfur (*chemistry*)
SBIR	Small Business Innovation Research
sccm	standard cubic centimeter per minute
SE	shielding effectiveness
Si	silicon
SiC	silicon carbide
SiO_2	silicon dioxide
SPM	Scanning probe microscopy
t	thickness
TiN	titanium nitride
TPa	terapascal
UV	ultraviolet

UHV	ultra-high-vacuum
U.S.	United States
V	volts
W	watt
Z_o	wave impedance of free space
Z_s	wave impedance of shielding material
Z_w	wave impedance of far field

List of Symbols

η	carrier density
μ	permeability of a material (*electricity*)
μ_0	permeability of a material (*electricity*)
μ_r	relative permeability (*electricity*)
μ_e	electron mobility
$\mu\Omega$	microOhoms
μ_h	hole mobility
μm	micrometer; micron
π	covalent bond; weaker than σ bonds
	a mathematical constant equal to approximately 3.14159
ρ	resistivity
σ	conductivity (*electricity*)
	covalent bond; strongest (*chemistry*)
σ_{Cu}	conductivity of copper (*electricity*)
σ_r	relative conductivity (*electricity*)
Ω	Ohms
λ	wavelength
ε	dielectric constant of a material
ε_r	relative dielectric constant of a material
ω	angular frequency
δ	skin depth (*shielding*)
%	percent

THIS PAGE INTENTIONALLY LEFT BLANK

EXECUTIVE SUMMARY

A rapid undertaking to exploit all potential avenues of use for graphene has been occurring since the scientific research and discoveries made by Geim and Novoselov in 2004 (Warner et al. 2013). Due to its extremely high value of electrical conductivity, a growing interest has also resulted in ascertaining if graphene may be suitable material for electromagnetic interference (EMI) shielding purposes. Researchers cited in 2012 that graphene was seven times more effective at EMI shielding than gold film. The research indicated that attenuation losses due to absorption overshadowed the losses due to reflection (Hong et al. 2012).

In an interest to continue to reduce the weight soldiers in the United States (U.S.) military bear, reducing the weight of portable electronics is one area of interest. According to Moore, the main factor contributing to the weight of portable electronics is the packaging needs to meet the stringent EMI shielding requirements specified in military standards. As noted on the Navy's SBIR website, The Department of Defense (DOD) is hoping that a graphene/polymeric composite will fill the capability gap that exists between metal electronic enclosures that satisfy a broad range of frequencies and conductive filled/coated plastics enclosures that have limited applicability (Moore 2011).

As described by Urlich and Eppinger, the first two phases of the product development process guide the efforts to determine if graphene can meet the DOD's needs. The planning phase will confirm that an opportunity exists. The concept development phase starts with identifying the customer's needs to understand the issue effectively and begin to build the target specifications (Urlich and Eppinger 2012). Once these two items are well established, concept generation and selection follow. Concept selection narrows down the concepts to those deemed viable for concept testing. Finally, the outcome of concept testing can hopefully provide data to support further investment into the product (Urlich and Eppinger 2012).

Information is collected to provide a substantive engineering background on topics associated with the endeavor. It is necessary to identify the current practices of

manufacturing graphene and how this process can be merged with the injection molding process and materials used to mold plastics. Electrical and mechanical characteristics of graphene are assessed. The governing principles that define the necessary shielding solution are also presented.

A concept generation table helps generate promising concepts. An examination of the product and system boundaries can aid in narrowing down the list. Modeling and simulation produce data to determine if the mechanical and electrical properties of graphene can provide substantial shielding effectiveness for the range of frequencies identified in Military Standard 461G, *Requirements for the Control of Electromagnetic Interference Characteristics of Subsystems and Equipment*.

Even though graphene exhibits a very high conductivity, its thickness (or rather its thinness) prevents it from being a good or excellent EMI shielding material. Simulations show that the reflection from the thin graphene layer is less than for a solid conductor. Furthermore, the attenuation of the field inside of the graphene is less than that of a metal conductor. In addition, graphene production is still categorized as fabrication of samples as opposed to mass or large-scale production.

References

Hong, Seul Ki, Ki Yeong Kim, Taek Yong Kim, Jong Hoon Kim, Seong Wook Park, Joung Ho Kim, and Byung Jin Cho. 2012. "Electromagnetic Interference Shielding Effectiveness of Monolayer Graphene." *Nature Nanotechnology* 5(8): 574–578.

Horton, Alex. 2017. "Army, Marine Corps Look to Lighten Load for Combat Troops." *Stars and Stripes*, May 17. https://www.stripes.com/news/army-marine-corps-look-to-lighten-load-for-combat-troops-1.468816#.WUsjjVFOn3i.

Moore, Donna. 2011. "Lightweight Electromagnetic Interference (EMI) Shielding System for Aircraft Avionics." (Navy SBIR 2011.2—Topic N112-097). *Navy SBIR*. Last modified May 26. http://www.navysbir.com/n11_2/N112-097.htm.

Ulrich, Karl T., and Steven D. Eppinger. 2012. *Product Design and Development*, 5th ed. New York: McGraw-Hill Irwin.

Warner, Jamie H., Franziska Schaffel, Mark Rummeli, and Alicja Bachmatiuk. 2013. *Graphene: Fundamentals and Emergent Applications*, 1st ed. Saint Louis, MO: Elsevier.

ACKNOWLEDGMENTS

The first person that I need to thank is Dr. David C. Jenn. The completion of this thesis would not be possible without him. I started this graduate program in the fall of 2012. I consider the product development program to be one of the best programs within the Systems Engineering Department at the Naval Postgraduate School (NPS). Initially, I had a hard time trying to find an advisor who was interested in graphene and its potential use for EMI shielding as the subject of my thesis. Within a few weeks, I finally found one. After about a year, I was approximately 60 pages into my draft when he informed me that he could no longer be my advisor. At that point, I had just filed my second thesis extension. I was living in Maryland and trying to contact professors in California to find an advisor. After seven months into my second extension, I finally reached out to the Electrical and Computer Engineering Department and contacted Dr. Jenn. Now, here I was deep into my thesis topic without an advisor. I can only imagine the thought that went through his head when I asked him. He agreed to be my advisor. He helped me file my third and final thesis extension. He agreed to pick me up and help me finish. I will always remember him agreeing to be my advisor as one of the countless blessings I have received in my life. Through numerous emails and phone calls, I am able to submit this thesis because of him. I hope he understands how deeply appreciative I am for his kindness and willingness to help me finish this program. He is the reason I am graduating.

When I started this program, I noticed classes in the NPS catalog that I wanted to take but was not offered within my program's schedule. So, since I live in Maryland, I looked to see if I could take some additional classes at the University of Maryland, College Park (UMD) to supplement my course work at NPS. I emailed some professors in the Mechanical Engineering Department at UMD to find out about some courses that would support the NPS Product Development curriculum. I emailed Dr. Michael Pecht about a reliability class that he was possibly teaching in the spring of 2013 and about the possibility of his being a co-advisor. I received a reply from him providing me

information on the course and he stating, “If you are asking me to be a co-advisor... that would be great ... I would be honored.” I still have that email to this day.

I had no idea that Dr. Pecht was the Director for Center for Advanced Life Cycle Engineering at UMD. I had no idea that he is recognized by the industry as a leading consultant in reliability engineering. I had no idea that he had received countless awards and honors. I had no idea that he had published hundreds of books and articles. If I had known all of this, I probably would have never contacted him. I would not have felt worthy. I would have easily convinced myself that he was too busy to have time for me simply seeking a master’s degree. I am the one who is honored to have him as my advisor. I can only hope that my performance in my future academic endeavors and professional career honors him for the time he dedicated to me. Thank you, sir.

I want to thank Professor John Green for ensuring that my thesis was molded in a way to provide a smooth process for it to be approved by the Systems Engineering Department Chair. I also want to thank Dr. Gary Langford. I thought I knew systems engineering until I took his class. I really struggled halfway through that class. I remember thinking that what he was talking about had nothing to do with engineering. Then the light came on, so to speak. What I learned in that class I have applied in every program or project that I have been involved with since. I keep his textbook from that class in my office.

I would like to thank the United States Marine Corps, which funded this education for me. I am completely thankful for this unbelievable gift. I wish to extend my sincere appreciation to all U.S. Marines who have served, are serving, and will serve.

Finally, I would like to thank Deb, Marie, and Landon, who had absolutely nothing to do with this thesis but everything to do with who I am. There is no job title, degree obtained, or level of status that I may earn or have bestowed upon me more important than having you in my life. At the end of the day, you are my home, and home is where my heart is.

I. INTRODUCTION

The information presented in this thesis attempts to probe the feasibility of synthesizing graphene production with injection molded, polymeric material while also determining if this combination can be an effective shielding material against electromagnetic radiation. A never-ending search is ensuing to lighten the load bearing on the United States (U.S.) soldier. The U.S. Army and the United States Marine Corps have been actively pursuing this goal. For example, the utilization of plastics to enclose batteries and ammunition containers has been implemented. Just recently, the Army released a request for proposals to design a new combat helmet that weighs 24% less than the current one (Horton 2017). However, a new helmet that weighs less but cannot provide the same level of ballistic protection would not suffice. Similarly, developing plastic enclosures of military electronics that fails at maintaining or further reducing the penetration of electromagnetic noise would not be useful either. The hope is that graphene can bridge the gap that currently exists between the current plastic composites and an actual metal enclosure. These benefits apply to other military platforms, such as ships and aircraft.

To guide this endeavor, Ulrich and Eppinger's use of a product development process is employed. A product development process defines the series of tasks that an organization or business generally follows to transform a thought or idea of a product to a manufactured good. In the early stages of the process, the tasks are more academic than tangible (Ulrich and Eppinger 2012). The undertakings of developing a product encompasses all the activities that start with identifying a need or want in a particular market and finishing when the purchase of that product is made by a consumer (Ulrich and Eppinger 2012). The remainder of this chapter touches on the activities of the planning phase and quickly moves into the first couple of steps of the concept development phase.

Figure 1 illustrates the generic model of the product development process that will used to assess the feasibility and the suitability of a graphene impregnated plastic material.

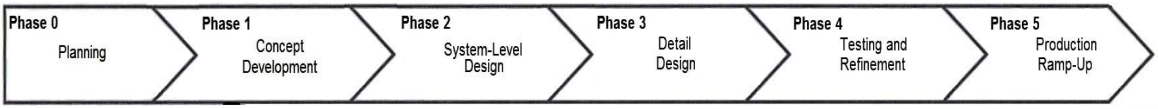

The generic product development process is an iterative, "stage-gate" progression (Dieter and Schmidt 2013, 37).

Figure 1. The Generic Product Development Process. Adapted from Ulrich and Eppinger (2012, 9).

According to Urlich and Eppinger, the early stages of product development begin with identifying an opportunity. An opportunity is a thought or concept that has a good chance of evolving into a new product or invention. An opportunity provides the initial eagerness to believe that pre-existing and emerging technology has given rise to a possible solution to an unmet need of a particular customer or industry. Opportunities are usually captured or documented in one page or less (Ulrich and Eppinger, 2012). The information usually consists of a sentence or two describing the new process or product, a brief description of how available resources and newly developed processes can deliver the desired outcome, and simple illustrations for additional clarity. It is during these brainstorming undertakings that many opportunities are identified with only the most viable ideas proceeding to more established product design and development processes. Karl Ulrich and Steven Eppinger (2012) state that one of the initial steps in the opportunity identification process is to "generate and sense many opportunities" to be followed by "screen opportunities" (Ulrich and Eppinger 2012). *Opportunity identification* is the first step in Phase 0 of the product development process shown in Figure 2.

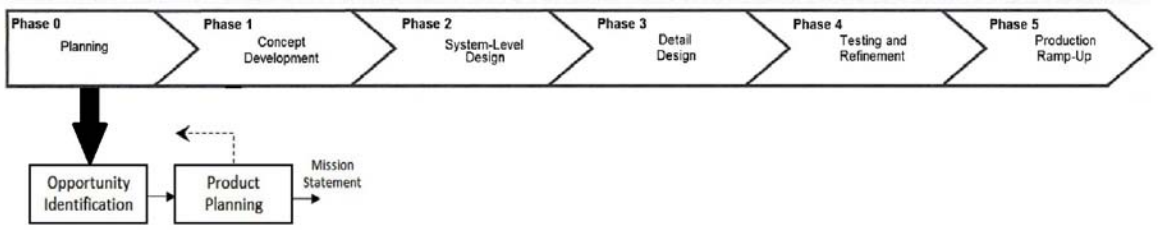

Figure 2. Phase 0, The Planning Phase, of the Generic Product Development Process. Adapted from Ulrich and Eppinger (2012, 9).

Opportunities have been identified for an improved electromagnetic interference (EMI) shielding material for advanced military electronics that can decrease the radiated electromagnetic emissions while also providing a significant weight reduction over commonly used shielding material. Traditional metals are commonly used as EMI shielding materials, and in certain applications, the use of composite materials that feature metal fragments encapsulated in a polymeric material. However, the metals add significant weight and corrosion concerns while the polymeric composites are only effective for a small window of frequencies. Therefore, the search for lighter weight materials with the EMI shielding effectiveness (SE) of metals is being conducted for modern, military applications (Moore 2011).

This opportunity is documented in academic explorations, such as Captain Benjamin Harder's thesis, "Evaluation of Nanocomposites as Lightweight Electronic Enclosures for Satellites' Applications" and Yücel Devellįoğlu's thesis, "Electronic Packaging and Environmental Test and Analysis of an EMI Shielded Electronic Unit for Naval Platforms." The Department of Defense (DOD) also funded numerous Small Business Innovation Research (SBIR) programs aimed at delivering the technology to satisfy the need for lighter weight EMI shielding material. SBIR Topic N112-097, "Lightweight Electromagnetic Interference (EMI) Shielding System for Aircraft Avionics," was issued for the V-22 Osprey Program in hopes of finding materials that will help reduce the weight of aircraft electronics while still providing the EMI shielding effectiveness required for each system..

As described by Ulrich and Eppinger, once an opportunity has been identified, the last step of the planning phase of the product development process is *product planning*. *Product planning* activities include, but are not limited to, evaluating and selecting which opportunities to pursue, establishing the potential or available markets for the product, and allocating resources for the endeavor (Ulrich and Eppinger 2012). This final step prepares the individual, team, or organization for the concept development phase by creating the mission statement that summarizes the directions to be followed (Urlich and Eppinger 2012).

A. IDENTIFYING CUSTOMER NEEDS

As defined by Ulrich and Eppinger, the next phase of the product development process is Phase 1, the concept development phase. In this phase, the system architecture is developed. The system architecture is formed from the information gathered during Phase 0 to define the composition and construction of the product better (Dieter and Schmidt 2013). The activities specific to the concept development phase of the product development process are indicated in Figure 3.

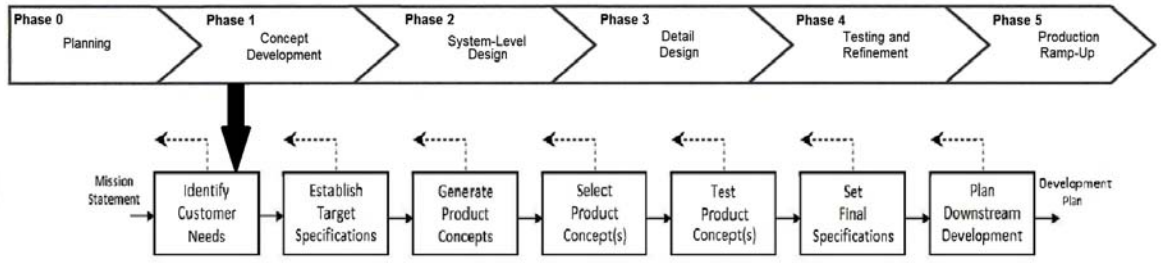

Figure 3. Phase 1, The Concept Development Phase, of the Generic Product Development Process. Adapted from Ulrich and Eppinger (2012, 9, 16).

With the mission statement in hand, the first step of the concept development phase is to *identify the customer's need* (Ulrich and Eppinger 2012). Ulrich and Eppinger's product development process indicates no difference exists between a need or want. The word *need* is simply used to label the features of a product that a customer

desires (Ulrich and Eppinger 2012). However, the DOD systems engineering process to identify the customer's need is to ensure that the customer has indeed stipulated a need rather than a want. The reason for this approach is that not all DOD customers are the actual end user. The soldiers and sailors are the predominant stakeholders in DOD acquisition. Therefore, the main purpose of DOD acquisition is to procure the necessary products that satisfy the end user needs as opposed to the needs of the customer, generally the DOD agency responsible for procuring the needs of the warfighter (DoDD 5000.01). Dieter and Schmidt (2013) make the same acknowledgment that to identify the needs of a new product fully and correctly, it is essential to explore those who impact or sway the customer stipulating the need (Dieter and Schmidt 2013).

Ulrich and Eppinger (2012) outline five basic steps to help an individual or organization identify customer needs:

- Collect information from the customer.
- Evaluate the information collected against the needs of the customer.
- Arrange the needs into a "hierarchy of primary, secondary, and if (necessary) tertiary needs" (75).
- Determine the importance of each need.
- Contemplate on the outcome and the manner in which the outcome was achieved.

Information has been collected from various sources to recognize a need for a lighter weight material for EMI shielding of DOD electronics. When attempting to evaluate the collected information against the distributed needs of the customer, additional questions arose in hopes of uncovering additional, unannounced needs that the enclosure would also have to satisfy. For example, is the equipment to be mounted and operated on an aircraft or a ship? Is the equipment to be portable or secured in a fixed location? An additional question may be, is the equipment to be operated indoor or outdoor, etc.? Additional end use conditions need to be considered to state the needs of

the customer fully. Environmental conditions, such as high and low-temperature operations, humidity, vibrations, and ballistic shock, can undeniably affect the material choice in an equipment enclosure. However, without having a specific customer at hand, the needs currently described at the beginning of this chapter can be used to form a shortened hierarchy of needs. The initial needs from the opportunities identified earlier may take the form listed in Table 1.

Table 1. Sample Hierarchical List of Primary and Secondary Customer Needs of a Lighter Weight EMI Shielding Material

Shielding material shall meet current EMI shielding requirements	• Shielding material must meet U.S. Navy (includes Marine Corps) shielding requirements for: o Aircraft o Ships o Submarines o Ground vehicles o Facilities • Shielding material must meet U.S. Army shielding requirements for: o Aircraft o Ground vehicles o Portable equipment o Facilities • Shielding material must meet U.S. Air Force shielding requirements for: o Aircraft o Ground vehicles o Facilities o Space
Shielding material shall be lighter than currently used enclosure material	• Shielding material density will be sizably less than steel • Shielding material density will be less than aluminum
Shielding material needs to be suitable for other environmental degradation	• Shielding material must resist corrosion • Shielding material must resist photodegradation caused by ultraviolet (UV) radiation

Once the hierarchy of needs has been assembled, the customer then distinguishes the relative importance of those needs, which is essential in guiding the product development team in determining which trade-offs to make and which resources to

allocate (Ulrich and Eppinger 2012). A customer survey is a very good instrument that can be used to gain information about the operations and environments of current products. The survey reveals the importance of each need for the redesign/improvement or may identify that a completely new product is needed (Dieter and Schmidt 2013). Table 2 shows a constructed survey to highlight the importance of the needs to the product development team.

Table 2. Example of a Product Design Survey. Adapted from Dieter and Schmidt (2013, 78).

	Response from Customer				
For this set of questions, place an X in the box under the heading that most accurately reflects your answer.	**Undesirable**	**Not Important**	**Nice to Have, Not Necessary**	**Highly Desirable**	**Critical**
Environment					
Shielding material needs to be suitable for UV exposure					
Shielding material needs to be corrosion resistance					
Shielding Frequencies					
Shielding for radiated emissions					
Shielding for radiated susceptibility					
Shielding for magnetic fields					
Shielding for electric fields					
Shielding for far fields					

For this set of questions, place an X in the box under the heading "YES" or "NO."	**YES**	**NO**
Is the equipment portable?		
Is the equipment stationary?		
Is the equipment to be operated on a ship – above deck?		
Is the equipment to be operated on a submarine or ship – below deck?		
Is the equipment to be used on ground/land based?		
Is the equipment to be used on Navy or Army aircraft?		
Is the equipment to be used on Air Force aircraft?		
Is the equipment to be used in space?		

Clarification	**Response**
How much should the density of the shielding material be in comparison to steel . . . ½, ¼, please provide.	
How much would you pay for a lighter enclosure compared to the cost of the current enclosure?	

Additional Comments

Dieter and Schmidt indicate that with the need acknowledged, arranged in a hierarchy, and prioritized, the outcome is then reflected as the preliminary sets of specifications begin to take shape. Tools, such as functional decomposition, quality function deployment (QFD), and heuristics, are used to translate the defined need or want of a customer and form a preliminary set of specifications to assist in the foundation of favorable concepts (Dieter and Schmidt 2013).

B. ESTABLISHING TARGET SPECIFICATIONS

Ulrich and Eppinger define target specifications as providing a more descriptive guide to the performance and constructional requirements of the product. The specifications restate the needs of the customer into technical provisions. Thresholds or objectives for the specifications are stipulated early in the product development process so that development team can have metrics by which to begin the *concept generation* step of the concept development phase (Ulrich and Eppinger 2012). During the generation of the concept(s), the specifications are iteratively updated or modified to consider constraints and additional derived requirements uncovered (Ulrich and Eppinger 2012). Table 3 illustrates an example of target specifications that may be set for seeking a lighter EMI shielding material for enclosing DOD electronics.

Table 3. Sample Target Specifications for a Lighter EMI Shielding Material

Requirement	Specification	Metric
Shielding material shall meet current EMI shielding requirements	DEFENSE PERFORMANCE SPECIFICATION: MIL-STD-461G, REQUIREMENTS FOR THE CONTROL OF ELECTROMAGNETIC INTERFERENCE CHARACTERISTICS OF SUBSYSTEMS AND EQUIPMENT	• Radiated Emissions tests RE101, RE102 and RE103 • Radiated Susceptibility tests RS101, RS103, and RS105
Shielding material shall be lighter than currently used enclosure material	PROGRAM-UNIQUE PERFORMANCE SPECIFICATIONS: This metric would be called out in the Performance Specification of each component or sub-system.	• New material shall have a density of ¼ or more than AISI 1018 steel. (≈7.87 g/cc) • New material shall have a density of ½ of aluminum. (≈2.70 g/cc).
Shielding material needs to be suitable for other environmental degradation	PROGRAM-UNIQUE PERFORMANCE SPECIFICATIONS: This metric would be identified in a Test Operating Procedure or Technical Manual referenced in the Performance Specification of each component, sub-system, or end product.	• The electronic enclosure shall perform without functional corrosion failures throughout its service life. Testing shall be conducted in accordance with (IAW) Internal Operation Procedure identified.
	DEFENSE PERFORMANCE SPECIFICATION: MIL-STD-810G, ENVIRONMENTAL ENGINEERING CONSIDERATIONS AND LABORATORY TESTS	• Laboratory Test Method 505.5, Solar Radiation 506.5, Rain 507.5, Humidity 509.5, Salt Fog

The objective of the thesis is carried out through the remaining steps of the concept development phase of the product development process. Chapter II dissects the problem and gathers information useful in solving the problem. This step will gather information on the recognized electrical and mechanical properties of graphene and the promising methods to produce it. The current polymeric injection molding processes are identified. The governing equations that ascertain a material's EMI shielding effectiveness are presented. Chapter III covers the steps of *concept generation* and *concept selection* to narrow down the viable concepts that continue to be refined. Chapter IV *tests* the concepts identified during concept selection to substantiate continued efforts, and hopefully, begin to shape the product specifications. This step conducts modeling and simulation of graphene to assess its EMI shielding effectiveness for military applications. The assessment starts with evaluating graphene's inherent shielding effectiveness to seeking graphene's probable shielding effectiveness when merged with a substrate. The last chapter closes with the final steps of *project planning*, *economic analysis*, and future work that takes the product into the system-level design phase of the product development process.

THIS PAGE INTENTIONALLY LEFT BLANK

II. REVIEW OF LITERATURE

Comprehending the performance of the products currently serving the customer and the new products that may potentially meet the customer's need is vital in the concept development phase of product development. Collecting information on products is attained by reviewing literature, relying on firsthand knowledge, and utilizing the disciplines of associated sciences and mathematics. The product is then dissected to understand the assembly of parts and choice of materials and to obtain ideas of how the product is fabricated. Dieter and Schmidt (2013) document four activities to dissect a product:

- Discover how the product operates or is intended to operate. What does the product do?
- Understand the science and engineering of how the product performs its functions. How does it do it?
- *Break down the functions of each subassembly and part.* How do the parts and subassemblies contribute to the function of the product? What are the boundaries between the parts?
- *How is the product is fabricated and assembled.* What are the processes and materials used to build the product?

A. CURRENT EMI SHIELDING MATERIALS

Surrounding an electrical device with a Faraday cage is the basic idea behind designing the enclosure for EMI shielding (Ott 2009). Enclosures are made of metals, conductive-coated plastics (coating the walls of the plastic enclosure via painting, metallic plating, or vacuum metallizing) or conductive-filled thermoplastic (a polymeric resin that is injection molded with conductive particles). The shielding enclosure must also take into consideration the mechanical and other electrical properties necessary for the system's operating environment. The material must also satisfy environmental

requirements, such as solar radiation, rain, humidity, extreme temperatures, and combat chemicals (Tong 2009).

1. Steel

Steel enclosures are chosen for their durability and very good fastener retention if threaded. However, it is the most difficult enclosure material to punch or machine. The corners and edges can easily be welded. However, with the use of steel, corrosion becomes an issue that requires the enclosure to be painted or coated. Steel enclosures increase the weight of the electronic system more so than aluminum or plastic (Design Innovation 2009).

2. Aluminum

Aluminum enclosures are used as EMI shielding enclosures due to their high conductivity. The low density of aluminum enables the enclosures to be the lightest metal material used for enclosing electronics; however, it is heavier than plastic and is the least durable metal enclosure. The use of aluminum lowers the risk of corrosion, but some operational environments require that the aluminum enclosure is processed (i.e., anodized) or coated. Threaded inserts are needed due to the poor thread retention ability of the metal (Design Innovation 2009).

3. Polymeric (Plastics)

Plastics provide for the lightest enclosure possible with no risk due to corrosion. Polymeric materials usually have an average fastener or thread retention with the ability to accept fastening inserts easily. The durability of a polymeric material can be affected by operational environment factors, such as humidity, temperature, and UV light exposure (Design Innovation 2009). However, because they are relatively low loss dielectrics, plastics provide little innate EMI shielding characteristics on their own. For a polymeric material to be suitable for EMI shielding, it needs to have a conducting agent, which is accomplished by either coating the walls of the polymeric enclosure with a conductive material or inserting conductive fillers into the plastic during the material's manufacturing process (i.e., injection molding or extrusion). With the application of

coatings, the shields tend to be thin. Coating the plastic is accomplished using conductive paints, flame/arc spray, vacuum metalizing, or electroless plating. A benefit is that an assortment of conductive materials can be used as opposed to aluminum and steel. However, the addition of a coating introduces new issues that must be mitigated. Reliability issues can occur due to delamination/adhesion problems when the enclosure is exposed to thermal cycling. Additional manufacturing cost associated with masking of the part and utilizing adhesion promoters can significantly increase the cost and lead times. Quality issues can occur during the manufacturing process that may scratch the coating, creating "slots" (shield failures). Even if the coating is integrated correctly, depending on the range of frequencies being generated by the enclosed electronics, it may not be an option that fully meets the shielding requirements of a product due to the thinness of the coating.

An alternative to coatings is the use of conductive fillers, which eliminates the additional steps of manufacturing associated with masking and coating applications. Also, conductive fillers can only be added to the plastic at 10% to 40% of the volume, which leaves "gaps" in the polymeric walls, and thereby limits certain bands of frequencies that the material is effective at shielding. Increasing the filler material any higher can significantly compromise the mechanical integrity of the material. Furthermore, the stress-strain relationship of a composite behaves differently in all axes as opposed to a homogeneous material. Additional analysis is required to ensure that the enclosure can withstand the mechanical loading determined by the operational environment (Ott 2009).

B. GRAPHENE

The carbon element, C, can take on different forms within the solid phase. The property of an element whereby it can exist in two or more different forms in the same phase of a given state is also known as allotropy. For example, in Figure 4, diamonds are constructed of carbon atoms arranged in a tetrahedral lattice arrangement. Amorphous carbon describes the arrangement of carbon that does not have any crystalline structure at all, which is represented in coal or soot. Another example of a carbon allotrope is

graphite. Graphite's carbon atoms, as shown in Figure 4, are stacked and bonded in a spherical formation. Graphene is simply another allotrope of carbon. This arrangement positions the carbon atoms in a lattice-type, hexagonal pattern. Graphene can be described as a layer of graphite a carbon atom thick (multiple layers of graphene bonded together form the carbon allotrope of graphite) (Warner et al. 2013).

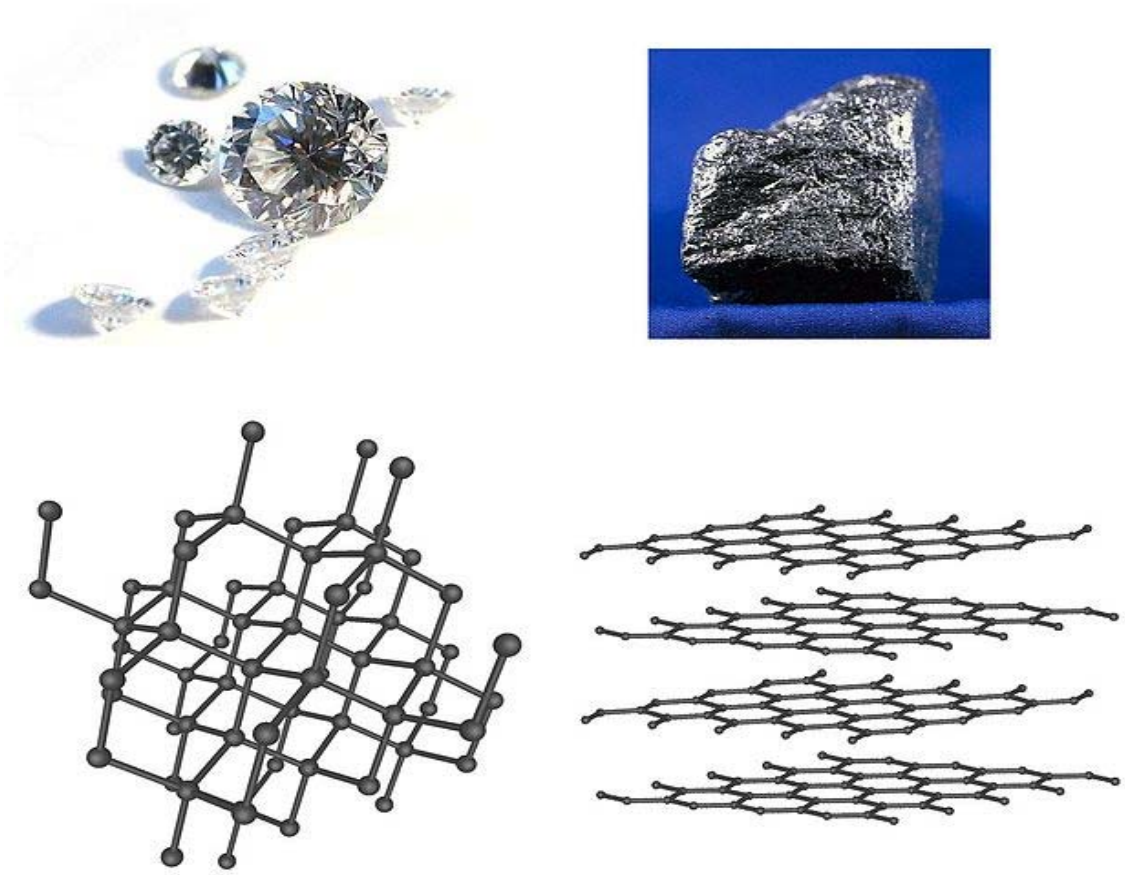

Figure 4. Structures of Different Carbon Allotropes. Source: *Wikimedia* (2014).

Two-dimensional (2D) crystal arrays separated from a three-dimensional (3D) specimen were thought to be nonexistent, as fluctuations in temperature of the environment of the 2D crystal arrangement would result in the melting of the structure. Experiments conducted in the pursuit of thin films have documented decomposition and

separation in structures with atomic thicknesses. However, in 2004, physicists at the University of Manchester and the Institute for Microelectronics Technology were the first to isolate individual graphene planes via micro-mechanical alleviation by simply attaching and removing adhesive tape to graphite (Warner et al. 2013). The efforts conducted at the University of Manchester led to Andre Geim and Konstantin Novoselow being awarded the Nobel Prize in Physics in 2010 for the development of graphene.

1. Electrical Properties

The electrical properties of graphene are explored, identified and compared with material associated with electronic packaging.

a. Conductivity

Electron mobility, μ_e, describes the characterization of how quickly an electron can move through a material when an applied electric field exists. Electron mobility is specified in units of $cm^2/(V•s)$. Conductivity is a measure of the ease with which a material conducts an electric current. In a mathematical expression, the conductivity, σ, of material is directly proportional to the material's electron mobility, μ_e, carrier density, η, and elementary charge, e. The elementary charge, e, is a constant equivalent to the charge of a single electron (1.602×10^{-19} coulombs (C)). In the case of semiconductors, they can have both electrons and holes. Therefore, hole mobility, μ_h, adds to the conductivity giving (Warner et al. 2013)

$$\sigma = e(\eta_e \mu_e + \eta_h \mu_h) . \tag{1}$$

For conductors, the equation can be expressed as (Warner et al. 2013)

$$\sigma = e\eta_e \mu_e . \tag{2}$$

Also, the reciprocal of conductivity, resistivity (ρ), is a parameter indicating a material's resistance to the flow of electrons (Warner et al. 2013),

$$\rho = \frac{1}{\sigma} . \tag{3}$$

Therefore, the most common electrical parameter for conducting materials is normally documented in units for conductivity or resistivity. Based on the relationship established in Eq. (2), it is not uncommon for two different materials to have the same conductivity but different electron mobility. One substance can have a small number of free electrons (carrier density) with high mobility for each, while another material comprises a large number of free electrons with small mobility for each. For metals, electron mobility is insignificant since the conductivity of most metals depends largely on the number of free electrons available. Therefore, mobility is relatively unimportant in metal physics.

In contrast to metals, electron mobility is a very important parameter for semiconductor materials. Generally speaking, higher mobility leads to improved performance (Warner et al. 2013). In regards to graphene, physicists at the University of Maryland have conducted experiments that indicate that graphene exhibits electrical attributes of both metals and semiconductors (University of Maryland 2008).

b. Intrinsic Properties

At room temperature, experimental data has revealed single-layer graphene to exhibit electron mobility as high as 200,000 $cm^2/V•s$, which results in a resistivity of about 1.0 μΩ•cm. This value is considered the intrinsic property of a single-layer of graphene. In Table 4, a compilation of several materials' resistivity, electron mobility, carrier density, and conductivity values are listed in comparison to the intrinsic value of graphene. Note that these are bulk or volume values, which can be significantly different than those for thin layers (i.e., surface conductivities) as discussed later.

Table 4. Electrical Properties of Common Materials at Room Temperature. Adapted from University of Maryland (2008); MatWeb (2015); Dow Corning (2014); Hurd (1972).

Material (from most conductive to least conductive)	**Resistivity (Ω·m) at 20°C**	**Mobility $cm^2/(V \cdot s)$**	**Carrier Density in $\times 10^{28}/m^3$**	**Conductivity (S/m) at 20°C**
Carbon (intrinsic graphene)	1.0×10^{-8}	$\mu_e = 200{,}000$		1.0×10^{8}
Silver	1.6×10^{-8}		6.96	6.5×10^{7}
Copper (annealed)	1.7×10^{-8}		11.71	5.9×10^{7}
Gold	2.2×10^{-8}		8.48	4.5×10^{7}
Aluminum	2.7×10^{-8}		18.2	3.7×10^{7}
Nickel	6.4×10^{-8}			1.6×10^{7}
Iron	8.9×10^{-8}		17.0	1.1×10^{7}
Stainless Steel 304	7.2×10^{-7}			1.4×10^{6}
Carbon steel (1018), cold drawn; *linearly extrapolated*	1.7×10^{-7}			5.8×10^{6}
Carbon (graphite)	6.0×10^{-5}			1.7×10^{4}
Carbon (diamond, natural)		$\mu_e \approx 2000$ $\mu_h \approx 1400$		
Silicon	1.0×10^{-4}	$\mu_e = 1900$ $\mu_h = 500$		1.0×10^{4}
Rubber, Natural, Not Vulcanized	1.0×10^{13}			1.0×10^{-13}
Polydimethylsiloxane (PDMS); Sylgard® 184	2.9×10^{12}			3.4×10^{-13}
Acrylic; polymethyl methacrylate (PMMA)	3.4×10^{13} (ave)			2.9×10^{-14} (ave)

Among natural materials, silver has the highest conductivity known at room temperature with an extremely low electron mobility, around 60 $cm^2/V\bullet s$. Comparing intrinsic graphene to silver, intrinsic graphene is approximately 54% more conductive than silver at room temperature. Silver has a far greater number of electrons than intrinsic graphene, but the graphene's conductive property is determined more by the fact that the electrons in intrinsic graphene are more mobile than those in silver are.

Initially, the focus of this research is to compare intrinsic graphene to metals normally associated with packaging electronics. Intrinsic graphene is roughly 2.9 times more conductive than aluminum, 14 times more conductive than carbon steel and close to

69 times more conductive than stainless steel. Note that all the metals in comparison to intrinsic graphene compare favorably to all the other allotropes of carbon. However, limitations arise because intrinsic graphene is only one atom thick and cannot provide the structural and mechanical properties needed for packaging electronics. Dr. Michael Fuhrer from the University of Maryland, College Park has stated that intrinsic graphene is so thin that it needs to be bonded or secured to another material. However, Dr. Fuhrer discovered that bonding graphene to another material affected the electron mobility within the graphene. In this manner, the graphene was categorized as extrinsic graphene with electrical properties dependent on the substrate to which it was attached. In the research conducted by Dr. Fuhrer, with graphene attached to a silicon dioxide (SiO_2) substrate, the electron mobility dropped from 200,000 $cm^2/V•s$ to around 10,000 $cm^2/V•s$ (University of Maryland 2008). This number equates to a conductivity of 5×10^6 S/m for extrinsic graphene on SiO_2 that puts it directly in the neighborhood of the conductivity of steel. Extrinsic graphene (with the proper substrate) is then still allowed to be a potential replacement for steel in packaging electronics.

The cause for the reduction of conductivity in the graphene was due to the trapped electrical charges in the silicon dioxide and atomic vibration of the SiO_2 atoms. The research pointed to a need to find better material to support intrinsic graphene structurally to reduce the scattering effects that limit the electron mobility in the graphene. Vacancies, which are a type of point defects, occur naturally in all crystalline materials, such as SiO_2. If intrinsic graphene can be bonded to a polymeric substrate, the electron mobility can be increased. An extrinsic graphene with an electron mobility of 70,000 $cm^2/V•s$ is comparable to aluminum (University of Maryland 2008).

2. Mechanical Properties

The mechanical properties of graphene are explored, identified, and compared with material associated with electronic packaging.

a. Physical Dimension

The atomic structure of carbon is comprised of the nucleus that contains six protons and six to eight neutrons depending on the isotope, and the nucleus is surrounded

by an electron cloud containing six electrons. The six electrons are arranged within the first (K) and second (L) shell of the carbon atom. The K shell contains two electrons, and the remaining four electrons occupy the L shell. The K and L shells are further arranged in sub-shells, s and p, and within each sub-shell, the electrons are further identified by their orbital and spin. Appendix B provides more details on the organization of electrons within an atom.

In carbon's lowest energy state, commonly referred to as the ground state, the six electrons are arranged in their shells, sub-shells, orbitals, and spin as $1s^2 2s^2 2p^2$ (Fuchs and Goerbig 2008). Figure 5 illustrates the ground and excited state configurations of the electrons within the carbon atom.

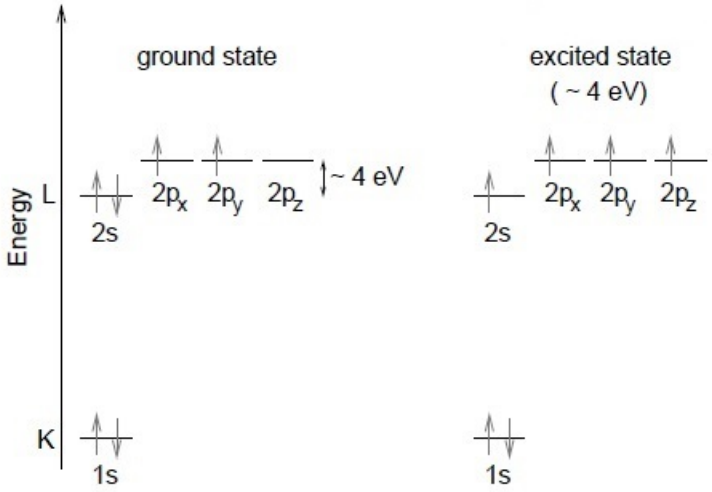

Figure 5. Electron Energy at Ground and Excited States for Carbon. Adapted from Fuchs and Goerbig (2008, 4).

However, one of the significant attributes of carbon is that when it comes in the vicinity of hydrogen, oxygen, or other carbon atoms, one of the electrons in the L shell's s sub-shell is excited to the final 2p orbital. This additional electron is now available for forming covalent bonds with additional atoms. In the excited state, the carbon atom now has four electrons in the L shell available for covalent bonding with other atoms. In some instances of bonding, carbon electrons exhibit hybrid orbitals (a mixing of orbitals). This

quantum-mechanical state of superposition between the s and p sub-shell electrons is called sp^n hybridization, which plays an essential role in covalent carbon-carbon bonds in graphene. Specifically for graphene, the carbon atoms exhibit the sp^2 hybridization. In the sp^2 hybridization, the electrons in the 2s orbitals mix with one electron from a 2p orbital to form three hybrid orbitals leaving one electron in the final p orbital (generally acknowledged as the p_z orbital). Figure 6 illustrates the sp^2 hybridization of carbon.

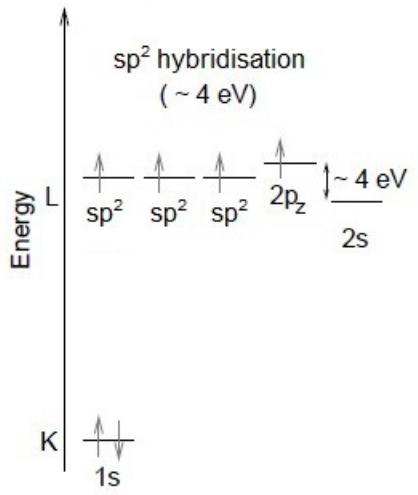

Figure 6. Electron Energy at the sp^2 Hybridization State for Carbon. Adapted from Fuchs and Goerbig (2008, 4).

Two types of covalent bonds are formed by the sp^2 hybridization, three sigma (σ) bonds, and one pi (π) bond. The σ bonds (sp^2 orbitals) are used to form the single and double bonds between the carbon atoms that create the benzene ring or lattice structure and set the distance between each atom (Fuchs and Goerbig 2008). The covalent bond length between two atoms should equal the sum of the two covalent radii. Since the σ bonds are between two carbon atoms, the carbon atom's covalent radii should be half of the σ bond length. The measured distance between the carbon atoms is 1.42 angstrom (Å), which is the average between the lengths of the single C-C bond (1.47 Å) and double (C=C) bond (1.35 Å). It should also be noted that the honeycomb shaped lattice is not necessarily a true hexagonal lattice. It is comprised of two intertwining triangular

sublattices. The closest atom to each atom in sublattice (A) is in sublattice (B). Conversely, the same is true for each atom in sublattice (B) to (A). The π covalent bond (p_z orbital), which is much weaker than the σ bonds, acts perpendicular to the graphene lattice. This bond is used to bind the graphene sheets to form graphite. This bond is longer and increases the thickness beyond just the covalent diameter of carbon established by σ bonds. The thickness of graphene is measured to be approximately 3.35 Å (Lee et al. 2008).

Figure 7 illustrates the triangular sublattice structure of the carbon atoms in graphene and the distances between the atoms.

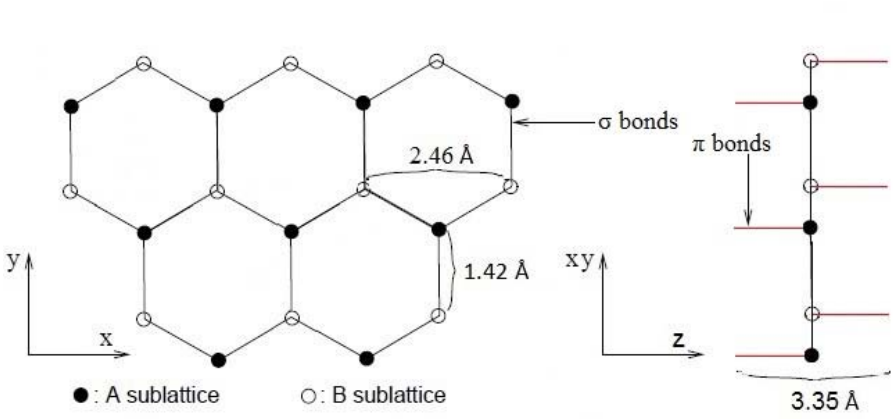

Figure 7. Sublattice Structure of Graphene with Distances (in Angstroms). Adapted from Fuchs and Goerbig (2008, 11).

Scanning probe microscopy (SPM) is a branch of microscopy that creates 3D images of nanoscale surfaces using a probe that physically touches the specimen. Figure 8 shows a SPM image of graphene developed by the U.S. Army Materiel Command (AMC). The p_z orbitals can be spotted as cone shaped protrusions extending perpendicular from the graphene sheet and centered on each nucleus of one of the triangular sublattices from this view.

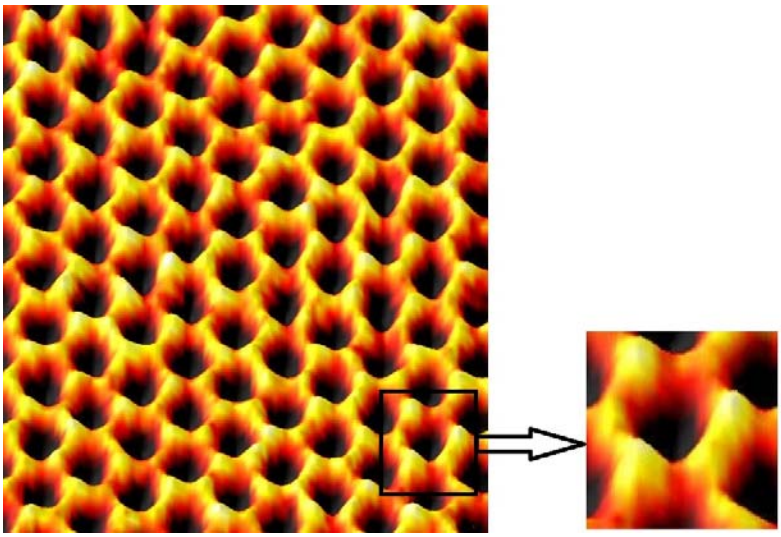

Figure 8. Scanning Probe Microscopy Image of Graphene. Adapted from U.S. Army Materiel Command (2012).

b. Strength

Since graphene is essentially an atom thick, it is generally viewed as a 2D material. The strain energy density has to be standardized to the area of the graphene sheet, as opposed to being based on the volume, as with normal substances. Therefore, its behavior under tensile loading is properly described by a Young's modulus and ultimate strength with units of force/length (Lee et al. 2008). Changgu Lee and associates discovered through experimentation that monolayer graphene had a breaking strength of around 42 N/m with a corresponding Young's modulus of E = 1.0 terapascals (TPa) with an associating intrinsic stress of roughly 130 gigapascal (GPa) at a strain of 0.25. If need be, these parameters can be divided by the thickness of graphene to acquire an approximate 3D parameter for comparing it with other materials. However, Lee et al. (2008) caution that, in doing so, those values are considered derived and not intrinsic to the monolayer; and therefore, restraint should be used when using those calculated values for comparative analysis. For example, Lee et al. discovered, at maximum curvature, that the energy from bending the monolayer was three times smaller than the energy from the in-plane strain, which conveys that the graphene membrane has essentially no bending stiffness. Based on those findings, and depending on the end-use application,

considerable thought must be applied when deciding to model graphene as a 2D or 3D substance and the mechanical properties associated with that model.

Nevertheless, comparisons between other materials still need to be made to determine if graphene can be a viable alternative for a given end-use application. For EMI shielding applications, a comparative analysis should be conducted between and steel. AISI 1018 cold-drawn steel, for instance, has an ultimate strength of 440 MPa = 4.40×10^{8} N/m^2 (MatWeb 2017). If the reverse approach is taken to derive the strength parameter in units of force/length of hypothetical steel film of the same thickness as graphene (graphene thickness can be taken to be 3.35Å=3.35×10^{-10} m), the 2D breaking strength of steel is calculated to an approximate range of 0.148 N/m. This simple comparison indicates that graphene is at least 283 times stronger than AISI 1018 cold drawn steel. This order of magnitude in strength can be very useful when assessing an enclosure's ability to withstand environmental conditions associated with shock and vibration.

3. Emerging Manufacturing Practices

Graphene's electrical and mechanical properties make graphene an ideal material suitable for thin, conducting films, such as touch screens and liquid crystal displays (LCD) (Warner et al. 2013). The electronic properties of graphene depend on the number of layers. Graphene is characterized as being a single-layer, bilayer, few-layer, or thin film (Warner et al. 2013). Typically, thin-film graphene is considered to be constructed using no more than ten layers of atomically thin graphene (Warner et al. 2013).

a. Mechanical Exfoliation

In 2004, the Manchester group that won the 2010 Nobel Prize in Physics attained graphene by mechanically separating layers of graphene from a mass of graphite. They used adhesive tape to split graphite crystals repeatedly into increasingly thinner pieces. The simple practice of writing with a pencil with graphite lead leaves layers of graphene behind on the paper. This practice of exfoliating graphene is relatively easy to perform and needs very little cost to perform. Many different methods of exfoliating graphene have been developed, including micromechanical exfoliation (adhesive tape), ultrasonic

treatment in solution (sonication), and milling. Even though obtaining graphene by the original method has been very successful, the yield and the quality of the graphene obtained are sporadic. The graphene tends to become "dirty" with contaminants from the exfoliating agent. The mechanical process similarly introduces strains and defects in the layers obtained. This drawback to the exfoliation process can lower or weaken the electrical properties of graphene. Sonication and ball milling have shown promise in producing a higher yield of single-layer or few-layer graphene, but the repeatability of the process to control the thickness has led to inadequacies, including minimizing the introduction of contaminates (Warner et al. 2013).

b. Epitaxial Growth on Metal Substrates

Chemical vapor deposition (CVD) is a chemical process conducted under high temperature to produce high-purity, high-performance materials. CVD is regularly employed in the production of thin-filmed semiconductors. The standard CVD process exposes a wafer (substrate) to one or more gaseous reactants that reduce and/or decompose onto the surface of the wafer to generate the anticipated residue. Various materials and metals are produced by this process. The yield of graphene on ruthenium usually is not uniform in thickness in terms of the graphene layers produced, while the bottom layer bonds strongly with the ruthenium, the next layer up is virtually detached and only faintly electrically connected to it (Mgrdichian 2008). In contrast, graphene grown on iridium is very weakly coupled, uniform in thickness, and well arranged, although graphene on iridium is somewhat rippled (Pletikosić et al. 2009). A few-layers of graphene of high quality have been created on nickel wafers using CVD by exposing the wafers to methane; The sheets of graphene created have been effectively relocated to other substrates, exhibiting a possibility for many electronic applications (Sukang et al. 2010).

Researchers at the University of Pennsylvania have since focused on three parameters of the CVD process to enable the growth of very thin, uniformly distributed graphene. Monolayers of graphene can be consistently produced (at a 95% yield) by selecting the best substrate material and controlling the surface finish of the substrate, in

addition to, adjusting and tuning the operating pressure of the methane (CH4) feed rate into the chamber (Zhengtang et al. 2011).

The research also considered a copper substrate to be more favorable in producing a thinner layer of graphene compared to other substrate material analyzed. One of the critical parameters of copper substrate was the surface finish. Electropolishing is a process utilized to reduce the irregularities on the copper surface. Copper foil was used as the substrate, and it had a thickness of 25 μm. The copper substrates were prepped by sonication in an acetic acid bath for five minutes to remove any oxide layers on the surface. The copper surface was polished initially with sand paper, then with a fine polishing paste, and finished with sonication in ethanol. The substrate was then allowed to dry. To begin the electropolishing process, the copper was placed into a 400 mL solution comprising 300 mL of 80% H_3PO_4 and 100 mL of ethylene glycol. A larger copper plate was placed in the solution to be used at the negative electrode. A voltage in the range of 1.0 to 2.0 V was applied across the copper anode and copper substrate for roughly 30 minutes. Quickly after the copper substrate was removed, the substrate was submitted to another sonication in a bath of deionized water. Any remaining acid was removed with 1% ammonia and washed again with ethanol. Finally, the substrate was blown dry with nitrogen gas. Atomic Force Microscopy images were taken before and after the electropolishing to determine and document the benefit gained by the additional polishing process (Zhengtang et al. 2011).

The CVD growth was conducted in a furnace with the copper placed in a quartz tube serving as the chamber. The chamber was cleared with argon (Ar) (600 sccm) and hydrogen (H_2) (10 sccm) for 10 minutes. Both gases continued to flow at the specified rates for the remainder of the graphene production. The furnace was heated to 800° C to anneal the copper for 20 minutes to again remove any oxides that may have collected on the surface. The furnace temperature was raised to 1,000° C, at which time the methane was introduced into the chamber. After the reaction time was reached, the chamber was positioned to a cool zone within the furnace and the flow of methane was stopped (Zhengtang et al. 2011).

Two methods of transferring the graphene from the copper substrate were attempted (Zhengtang et al. 2011):

- PMMA method: A thin film (≈300 nm) of polymethyl methacrylate (PMMA) was spin-coated on the layer of graphene (polished side) produced on the copper foil substrate. The resin was baked at 160° C for 20 minutes to allow the solvent to vaporize. Graphene on the unpolished side of the copper film was detached by oxygen reaction ion etch (RIE) at a power of 45 W for about two to five minutes. The combined substrate and graphene sample were placed in a solution of 0.05 g/mL iron chloride at a temperature of 60° C with the PMMA side down. The copper was slowly etched from the graphene over the course of three to 10 hours (Zhengtang et al. 2011).

- PDMS method: A polydimethylsiloxane (PDMS) stamp was used to transfer the graphene from the copper substrate. PDMS epoxy was composed of 20 parts of Sylgard 184 prepolymer and one part curing agent by weight. The solution was mixed vigorously for two minutes until bubbles filled the mixture. The bubbles were extracted by placing the solution in a vacuum. PDMS epoxy was poured onto the graphene (polished side) and cured in a vacuum for one hour at a temperature of 70° C. Removing the graphene from the backside of the copper substrate is identical to the process specified in the PMMA application (Zhengtang et al. 2011).

c. Dry Ice Method (Carbon Dioxide Reduction Method)

Burning magnesium (Mg) metal in the presence of carbon dioxide (CO_2) produces carbon,

$$2Mg(s) + CO_2(g) \rightarrow 2MgO(s) + C(s). \quad (4)$$

Until recently, the chemical reaction for manufacturing a solid, nanostructured sample of graphene has not been widely reported. Researchers at Northern Illinois

University delved into this approach to provide further incentives for a "greener" method of manufacturing graphene (Chakrabarti et al. 2011).

Three grams of Mg strips was burned inside a dry ice bowl in an environment of CO_2. After the combustion reaction was finished, the black residue was gathered and placed in a beaker containing 100 mL of 1 M hydrochloric acid (HCl). The solution was mixed overnight and maintained at room temperature to eradicate the MgO product and any residual Mg that did not fully combust. Both of these contaminants react with HCl to form the solid compound $MgCl_2$. This compound is dissolvable in water, leaving pure carbon. The mixture was washed and filtered with deionized water numerous times to neutralize the pH level. Finally, the graphene was isolated and dried overnight in a vacuum at 100° C. The yield was calculated to be 92% (Chakrabarti et al. 2001).

The distinct process of the materialization of graphene is still being determined, but the elevated temperature created during the burning of the magnesium metal is thought to play a key role. It is speculated that the combustion of the solid Mg in the gaseous CO_2 promotes the quick production of graphene. The reaction time needs to be longer to form multiple layers of graphene. Due to the kinetics of the carbon atoms, only few-layer graphene is favored (Chakrabarti et al. 2001).

d. Epitaxial Graphene on Silicon Carbide

Research was conducted at Carnegie Mellon University to generate graphene by heating silicon carbide (SiC) to very high temperatures (>1,100° C) under low pressures (~10^{-6} torr) (Luxmi et al. 2009). Since SiC has a comparatively large band gap compared to most semiconductors, graphene mechanisms functional at room temperature can be constructed exactly on top of it. As for carrier mobility, the electrical parameter used to indicate high quality of graphene, greater values are conveyed for graphene fabricated on SiC than for graphene grown by CVD. Single, monolayers of graphene produced by thermal decomposition of SiC could be the basis for mass production of graphene integrated devices (Hibino et al. 2012).

A graphite strip heater was placed in an ultra-high-vacuum (UHV) chamber. The base pressure was set at 1×10^{-10} Torr. Two vacuum pumps were used, a turbo-molecular

pump rated at 150 l/s and a “hydrogen-getter” pump. A rectangular, graphite plate having an area of 7,500 mm^2, 1-mm thick, was cut into a bow-tie shape. The bow-tie was dimensioned with a narrow neck of 20 mm length and 14 mm width. A transformer provided power to the graphite strip heater capable of supplying up to 1323 watts. Current (up to 210 Amperes, A) was supplied by two, 9.5 mm-diameter copper conductors. The water-cooled conductors were held in place by large copper clamps on the two 75-mm ends of the plate. Gate valves separated the turbo pump and the “hydrogen-getter” pump from the main chamber. During the H_2 etching, the gate valves were closed and the turbo-pump was switched off. For graphitization, the gate valves were opened when the turbo-pump was switched on (Luxmi et al. 2009).

The experiment was performed on 4H-SiC samples. As obtained, both sides of these substrates had been polished with the (0001) side receiving further polishing. The surface finish of the SiC used for graphene formation greatly influenced the electron mobility and thickness of the graphene. Square test samples having an area of 100 mm^2 were cut from the wafers. Hydrogen-etching was conducted at 1 atm pressure using pure hydrogen gas flowing at 10 lpm. The hydrogen-etching was conducted for three minutes at a temperature of 1,550 °C to eliminate scratches. Temperature was recorded using a disappearing filament pyrometer. Even though the pyrometer was pointed directly at the sample, the temperature recorded was mostly that of the heater strip due to the transparency of the sample. Once the H-etching was completed, the turbo-pump was restarted and the gate valve to the “H-getter” pump was opened soon after. After approximately 30 minutes, the pressure in the chamber reached 1×10^{-8} Torr. The annealing to form the graphene was performed. The annealing process occurred at temperatures ranging from 1,100–1,500° C. This process causes the thermal sublimation of silicon. Silicon was removed from the SiC surface using thermal sublimation leaving behind graphene form from the extra carbon (Luxmi et al. 2009).

To remove the graphene from the SiC wafer, a sublimation process can be used. The transfer starts with coating the graphene/SiC sample with a layer of silver, Au, approximately 100 nm thick. The layer of silver was followed by a layer of polyimide/ amic acid solution. The SiC substrate was spun at 3,000 rpm for half a minute and then

heated at 110° C for two minutes to evaporate the solvent. The two-minute duration moderately cures the epoxy. The bilayer film of gold/polyimide was peeled away from the SiC wafers, which lifted the graphene off the wafer. The graphene can then be transferred to another substrate, typically silicon or SiO_2, by oxygen plasma reactive ions etching away the gold/polyimide bilayer (Unarunotai et al. 2009).

C. POLYMERIC INJECTION MOLDING PROCESS

In the injection molding process for polymeric materials, a large amount of the plastic is held in the heating chamber, and a small amount is injected into the closed mold, which is typically referred to as the tooling. For thermoplastic material, the tooling temperature is kept low to promote "chilling" or hardening of the polymeric material after it is injected. When thermoset materials are used, the tooling temperature is hotter to finish the curing process. Depending on the polymeric material being molded, the temperature of the cavity is lowered to the demolding temperature prior to ejection. The final part can be ejected by cams and levers automatically operating the tooling pieces, or the tooling can be manually removed from the injector press where the part can be separated from the cavity (Buckleitner 1995).

1. Mold Material

The processing machinery, production requirements, and the polymeric resin being processed all contribute to the selection of the material used to construct the injection mold (generally referred to as the tooling).

a. Steel

Steel is typically used to provide reliable functioning molds with long service life cycles. Steel provides a large selection of alloys and grades capable of being subjected to several surface treatment processes. Some types of steel permit economical machining and capacity for ease of heat treatments, while some types of steel are difficult to polish and have resistance to additional surface finishes. Steels with strengths in the range of 600 to 800 MPa can be easily machined, while steels above 1,500 MPa start to become difficult to manipulate. Types of steel of less than 1,200 MPa need additional surface

treatment, such as hardening and tempering to meet the demands of injection molding. Sulfur can be added to steel to pre-harden the material while still retaining the ease of machining but cannot be polished well and are prone to corrosion. Heat-treating the steel tooling after machining must be done with care to prevent rendering the mold unusable due to distortion. The melting temperature of common thermoplastics is around 400° C, which can require the tooling temperature in the injector press to be kept at around 200° C. The steel tooling would have to resist creep and fatigue from the thermal cycling environment of polymeric part making (Menges and Mohren 1993).

Surface treatment of steel tooling is done to provide a particular surface finish, reduce fatigue and wear, minimize corrosion, and promote the formation of material residues and deposits in the mold. The tooling surfaces can be heat-treated through processes, such as annealing, hardening, and tempering. Some polymeric materials release harsh gases that require electrochemical treatment of the steel surface, such as chrome plating or nickel plating to prevent corrosion or pitting of the surface. Surfaces can also be chemically etched to add texture and features for aesthetics. The surfaces can be enriched with carbon, nitrogen, and boron through carburizing, nitriding, and boriding, respectively. This process can be carried out through the CVD process. The CVD process occurs at temperatures between 800° C and 1,100° C. The deposits precisely copy the surface of the mold to include imperfections and surface defects. The high temperatures can cause the steel tooling to lose hardness and strength, which may need to be compensated for by repeating the heat treatment and hardening process. Care should be used when selecting a steel tool for the CVD process.

Instead of the CVD process, physical vapor deposition (PVD) is used to deposit solids on the tooling by thermal and kinetic energy bombardment in a vacuum. The PVD process takes place at temperatures (500° to 550° C) much lower than CVD. This temperature is lower than the tempering and hardening temperatures used to prepare the surface of the tooling. The quality and cleanliness of the tooling surface are crucial for proper adhesion of the coating being applied. So far, only titanium nitride (TiN) layers around 5 μm thickness have been applied to steel tooling by the PVD method (Menges and Mohren 1993).

b. Zinc

High-grade alloys of zinc are mostly used for molding prototypes or low production runs due to the substandard mechanical properties when compared to other tooling materials. Zinc alloys are used for blow molding and vacuum forming. Tools made of zinc are mostly cast. For this research, zinc is not considered for injection molding as a graphene substrate (Menges and Mohren 1993).

c. Copper

Beryllium-copper alloy is used for injection molding with a minimum composition of 1.7% beryllium and 97.3% copper. The beryllium content usually does not exceed 2.5%. This alloy has a tensile strength up to 1,200 MPa and can be surface hardened. The material is very ductile and polishes well. The material is corrosion resistant and suitable for electrochemical plating, mostly nickel (Menges and Mohren 1993). Figure 9 lists the top designations of beryllium-copper for mold construction.

Table 4.14 Beryllium Copper Alloys; Properties and Applications.

Designation	*Composition (Balance Cu)* Be	Co	Others	*Thermal Conductivity (BTU/ft/hr/°F at 68°F)*	*HRC**	*Characteristics and Applications*
C172000	2.0	0.5		60	40	Good strength and wear resistance with good electrical and thermal conductivity
C17510	0.6	2.5		145	22	High thermal and electrical conductivity but lower hardness. Used where maximum heating and cooling rates are essential
C82400	1.7	0.3		58	37	Good strength, hardness, corrosion resistance, and conductivity
C82510	2.0	0.5	0.3 Si	56	41	Similar to 82400 above, but with better castability
C82600	2.3	0.5	0.3 Si	54	44	As 82400 above, but with improved wear resistance. Used in pressure and Ceramic Casting
C96700	1.2		30.0 Ni	21	50	Highest corrosion resistance and strength and castability, but lower thermal conductivity. Resists flame retardants, blowing agents and other corrosive chemicals contained in molding resins

*HRC—Hardness Rockwell C

Figure 9. Properties of Beryllium-copper Alloys.
Source: Buckleitner (1995, 140).

d. Aluminum

Aluminum alloys 7075-T6 and 7029-T6 are used in aircraft construction and have been utilized in injection mold tooling. The ease of milling and the high thermal conductivity are properties highly valued in injection tools. Aluminum is lighter than steel, but the reduced strength requires the tooling to be about 40% thicker. Tooling is less prone to distortion from the machining process due to less residual stress as compared to steel (Menges and Mohren 1993).

2. Mold Design

The mold design encompasses the tooling that forms the physical boundaries of a part and the additional features of the mold that work in association with the injection molding machine (IMM) to produce the part. In the mold design, stationary and moving

parts are utilized in forming the many features of a molded part, such as bosses, ribs, and openings (Rosato, Rosato, and Rosato 2000). Operations of the mold can range from being totally automatic to completely manual. Depending on the mold design, mold operations can be semi-automatic requiring some manual operation of the tooling. Those operations performed by the IMM are considered primary operations. Post-molding operations, such as ultrasonic welding, machining, and polishing, are considered secondary operations.

In the simplest of mold designs, the mold is made of two parts that contain the cavity and the core to comprise a polymeric injection mold. The location of the cavity is generally the stationary side of the mold. The cavity is where the injection of the plastic occurs. The core part of the mold is built into the moving side of the mold. The parting line is the location of the plane at which the two parts of the mold meet. A single nozzle would direct the molten polymer into the mold's sprue opening. A sprue, generally located within a bushing, would then direct the flow of the hot plastic into the mold. Vents designed within the mold halves would allow the release of trapped air or gases as the molten polymer filled the mold. Once the mold has been filled, water channels that are cut and designed into the mold are then used to control the cooling of the polymer to an inflexible state. Once the plastic part has solidified, the two halves of the mold are separated. The molded part is released from the cavity by adhering itself to the core, and the final part is released from the core by the use of ejector pins. This simple mold design is illustrated in Figure 10.

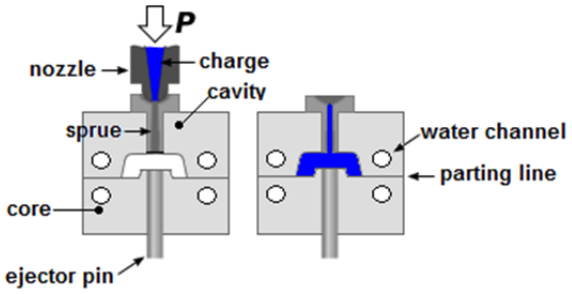

Figure 10. Simplified Diagram of an Injection Mold Design.
Adapted from *Wikimedia* (2016).

Also, a single mold design can be used to produce multiple parts, as shown in Figure 11. The mold design must include runners and gates to convey and control the flow of molten plastic from the sprue to the additional cavities.

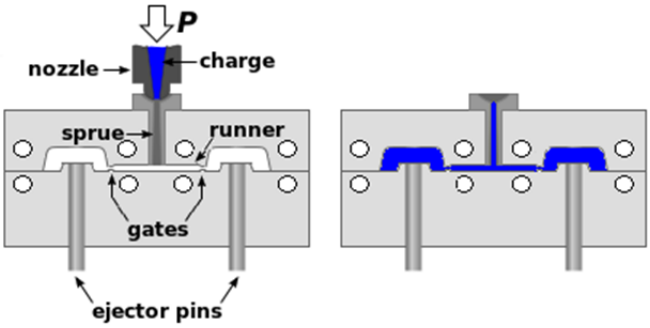

Figure 11. Injection Mold with Runners and Gates.
Adapted from *Wikimedia* (2016).

The mold design can become more complicated if an attempt is made to reduce or eliminate secondary operations by moving those part features to the primary operation of the IMM. Secondary operations use sliders, or pins, that move perpendicular to the core's movement. These features cannot be easily formed under the normal operating action of the mold's core and therefore require the addition of manual operations. This additional need would force constraints on the other design features mentioned in a simple mold design (Rosato, Rosato, and Rosato 2000).

3. Injection Molding Machine

The basic function of the IMM is to push molten plastic material into a comparatively cool mold to manufacture a product or part. The IMM is made up of two sections, the injection unit, and the clamp unit. The cavity part of the mold is mounted into an injection unit. The injection unit comprises the heating cylinder, often called a barrel, which melts the incoming plastic to an operational temperature. The hopper stores and feeds, typically by force of gravity, the polymeric resin pellets into the heating

cylinder. Inside the heating cylinder, the molten plastic is pressurized and delivered to the mold using a metering screw and nozzle (Bryce 1996).

The clamp unit is the section of the IMM where the core part of the mold is attached. The main component of the clamp unit is the clamping mechanism, which provides the force to keep the mold closed against the injection pressure created by the metering screw in the injection unit. The ejection mechanism is also housed within the clamp unit (Bryce 1996). Figure 12 displays a simplified representation of an IMM.

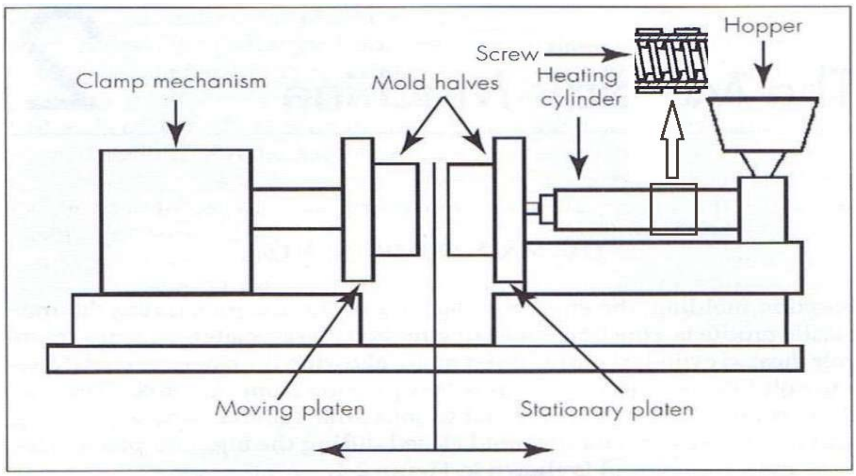

Figure 12. Simplistic Diagram of an IMM. Adapted from Bryce (1996, 12).

D. EMI SHIELDING

Shielding is the method utilized to contain electromagnetic radiation in an area from propagating into another area. It can also be used to prevent electromagnetic radiation from entering an area where none exists. The shielding is typically constructed from a conductive material, usually a metal. The effectiveness of the shield depends on the material used, the material thickness, and the frequency of the fields in relation to an incident electromagnetic field. In cases in which a conductive enclosure, also known as a Faraday cage, is needed to block electrostatic fields, the size of the shielded volume and the size, shape, and orientation of apertures become additional factors that need to be considered (Ott 2009).

1. Near Fields and Far Fields

As documented by Ott (2009), a field's attributes are established by the location of the radiation source, the material that surrounds the source, and the distance between the source and an arbitrary observation point in the surrounding material. The closer the observation point is to the source, the more closely the field properties are tied to the source properties (Ott 2009). The farther away the point moves from the source, the more influential the material surrounding the source becomes on the field properties (Ott 2009). Thus, the areas closer to the source are termed near fields or induction fields, and the areas farther from the source are considered the far or radiation fields (Ott 2009). The near and far fields are determined by the transitional region established by the relationship of the wavelength (λ) of the radiated source divided by 2π, as shown in Figure 13.

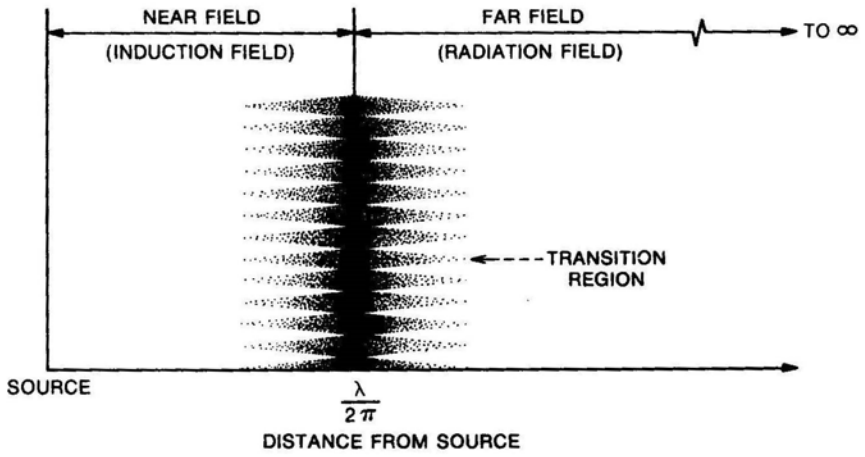

Figure 13. Near Field and Far Field Regions Transitioning from an Electromagnetic Source. Source: Ott (2009, 240).

The wave impedance of an electromagnetic wave is the ratio of the electric (E) and magnetic (H) fields. The wave impedance is represented by the symbol Z_w and is expressed in units of ohms (Ott 2009),

$$Z_w = \frac{E}{H}. \tag{5}$$

In the far field, this ratio matches the impedance of the medium through which it is passing. For free space or air, this ratio equals 377 Ω (Ott 2009).

Ott (2009) states that in the near field, the ratio between *E* and *H* is determined predominantly by the source. If the source is predominantly electric, then the electric field weakens at a rate of $(1/r^3)$ from the source as the associated magnetic field weakens at a rate of $(1/r^2)$ (see Figure 14). As the observer moves further from an electric source and approaches the transition region, the wave impedance decreases (Ott 2009). A short dipole antenna is an example of an electric source. The opposite can be stated for a primarily magnetic source. The magnetic field weakens at a rate of $(1/r^3)$ from the source as the associated electric field weakens at a rate of $(1/r^2)$ (Ott 2009). A small loop antenna is an example of a magnetic source (Ott 2009).

So, as the wave travels away from the source approaching the transition region, the wave impedance increases. In the far field, both the electric and magnetic fields diminish at a rate of $1/r$ (Ott 2009). Figure 14 graphically explains the relationship of the wave impedance as an observer travels from the near field region into the far field region of a given electromagnetic source.

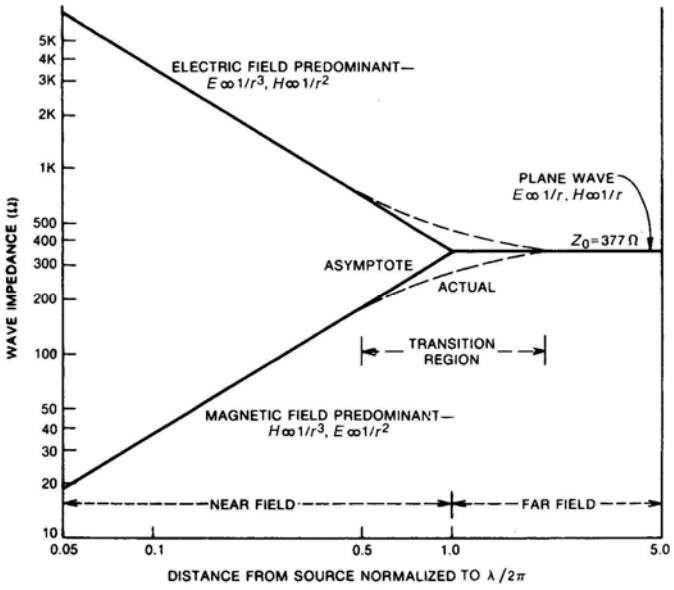

Figure 14. Wave Impedance Relationship to the Distance from the Source. Source: Ott (2009, 241).

Since the ratio between the electric and magnetic fields is irregular in the near field, the electric and magnetic fields must be evaluated individually. However, in the far field, the wave impedance is constant, and eventually both fields combine to form a plane wave (Ott 2009).

2. Wave Impedance

When the plane wave travels through the walls of an enclosure, the wave impedance of the plane wave is influenced by the impedance of the medium in which it travels, which leads to the wave impedance expression (Ott 2009)

$$Z = \sqrt{\frac{j\omega\mu}{\sigma + j\omega\varepsilon}}, \tag{6}$$

where

- μ is the permeability of the enclosure's material expressed in units of H/m
- ε is the dielectric constant of the enclosure's material expressed in units of F/m
- σ is the conductivity of the enclosure's material expressed in S/m
- ω is the angular frequency
- j is the imaginary unit

The symbol for the impedance of free space is Z_o. In the far field, the wave impedance, Z_w, equals the free space impedance, Z_o. Using the conductivity of air, which is essentially zero ($\sigma \approx 0$), Eq. (6) gives (Ott 2009)

$$Z_0 = \sqrt{\frac{j\omega\mu_0}{j\omega\varepsilon_0}} = \sqrt{\frac{\mu_0}{\varepsilon_0}} = 377\ \Omega. \tag{7}$$

For conductive material ($\sigma >> j\omega\varepsilon$), the impedance of the material of the enclosure is called the shield impedance, Z_s. The expression becomes (Ott 2009)

$$Z_s = \sqrt{\frac{j\omega\mu}{\sigma}} = \sqrt{\frac{\omega\mu}{2\sigma}}(1 + j), \tag{8}$$

$$|Z_s| = \sqrt{\frac{\omega\mu}{\sigma}}. \tag{9}$$

Through substitution, the shield impedance for any conductive material can be determined by the simplified expression (Ott 2009)

$$|Z_s| = 3.68 \times 10^{-7} \sqrt{\frac{\mu_r}{\sigma_r}} \sqrt{f}. \tag{10}$$

The representative value for relative permeability, μ_r, and conductivity relative to copper, σ_r, is discussed in Section 3.

3. Characteristic Constants

Permeability, in the realm of electromagnetism, is a characteristic of a material that quantifies how easily a material can be magnetized. The ratio that exists between the intensity of a magnetic field and the associated flux density is a constant. (Stanley and Harrington 1994). It is usually represented by the symbol, μ. For free space, $\mu = \mu_0$, and for other material, $\mu = \mu_r\mu_0$, where μ_r is the relative permeability. The permeability of most materials is very close to free space, which means that the relative permeability of most materials is close to 1. For ferrous metals, however, the value of μ_r may be several hundred (Stanley and Harrington 1994). Although attempts to discover or establish magnetic properties for graphene are currently underway, these attempts are in their infancy; therefore, intrinsic graphene will default to $\mu_r \approx 1$.

With the definition of conductivity having been established in Chapter I, relative conductivity, σ_r, is simply a ratio of a substance's conductivity to the conductivity of copper (annealed); $\sigma_r = \sigma_{Cu}/\sigma$. For this reason, the relative conductivity of copper (annealed) is equal to 1 (Ott 2009). The values for relative permeability and conductivity are captured in Table 5.

The dielectric constant, or permittivity, of a material is $\varepsilon = \varepsilon_r\varepsilon_0$; however, it rarely is needed due to shielding equations being defined as a function of the electromagnetic wave's frequency, as shown in Eq. (10) (Ott 2009). If graphene is attached to a substrate, then the substrate's ε_r affects the reflection loss, generally increasing it.

Table 5. Relative Conductivity and Permeability of Shielding Material. Adapted from Ott (2009, 243).

Material	σ_r	μ_r
Graphene (intrinsic)	1.69	1
Silver	1.10	1
Copper (annealed)	1.00	1
Gold	0.76	1
Aluminum	0.63	1
Nickel	0.20	100
Steel (SAE 1045)	0.10	1000
Stainless Steel 304	0.02	500

4. Shielding Effectiveness

With the exception of apertures, shielding effectiveness is analyzed with a transmission line model. As with transmission lines, loss and reflection components need to be considered for an enclosure. The heat generated within the enclosure is associated with the loss, while the difference between the impedance of the incident wave and the enclosure's impedance accounts for the reflection (Ott 2009).

Shielding effectiveness is commonly measured in decibels (dB). A logarithmic expression for decibels is (Ott 2009)

$$dB = 10\log\frac{P_2}{P_1}. \tag{11}$$

A positive decibel from this expression indicates a power gain ($P_2>P_1$) while a negative number indicates a power loss ($P_2<P_1$). The relationship of taking the log of a division of two numbers is simply the difference of the log of those individual numbers as (Ott 2009)

$$\log\left(\frac{a}{b}\right) = \log a - \log b. \tag{12}$$

This basic equation represented in Eq. (11), when modified for its use for shielding effectiveness (*SE*) in terms of the electric fields (Ott 2009) is

$$SE = 20\log\frac{E_0}{E_1}, \tag{13}$$

and for magnetic fields (Ott 2009) is

$$SE = 20\log\frac{H_0}{H_1}. \tag{14}$$

The incident field strength is represented by E_0 (H_0) while the field strength of the wave emerging from an enclosure is represented by E_1 (H_1).

The design of an enclosure must focus on two major factors concerning shielding effectiveness. The first factor is the material of the enclosure. The other is breaks, or apertures, in the enclosure resulting from the assembly of switches, connectors, displays, and with moving parts of the enclosure itself, such as lids or doors. It is extremely difficult to model or simulate apertures that develop from the packaging of electronics. However, an innate aperture of graphene due to its lattice structure needs to be analyzed in conjunction with the shielding effectiveness of the material. Graphene needs to be assessed on its shielding effectiveness as a solid shield first, and the effects of the lattice openings are then considered. The openings in the lattice structure at high frequencies decide the overall effectiveness of graphene as an EMI shield (Ott 2009).

5. Shielding Material

A solid material (generally a metal or a material having a metallic surface) can have its shielding effectiveness calculated by the following expression (Ott 2009):

$$SE = A + R + B \ \text{(dB)}, \tag{15}$$

where

- A is the absorption loss
- R is the reflection loss
- B is the correction factor to account for multiple reflections in thin shields.

All terms have to be in units of dB. When the absorption loss, *A,* is greater than about 9 dB, the multiple reflection factor becomes negligible. For electric fields and plane waves, the *B* factor is also considered negligible (Ott 2009).

Through derivations and substitutions, Henry Ott provided the following universal expression for calculating absorption loss given a material thickness, *t*, as (Ott 2009)

$$A = 3.34t\sqrt{f\mu_r\sigma_r}\ . \tag{16}$$

This equation shows that the absorption loss is proportional to the thickness of the material (inches) and exponentially proportional to the frequency (Hertz) of the electromagnetic wave passing through the enclosure and the relative permeability, μ_r, and conductivity, σ_r, of the enclosure material (Ott 2009).

Ott (2009) provided a generalized equation for reflection loss as

$$R = C + 10\log\left(\frac{\sigma_r}{\mu_r}\right)\left(\frac{1}{f^n r^m}\right). \tag{17}$$

The constants *C*, *n*, and *m* are identified in Table 6.

Table 6. Constants to Be Used in Eq. (17). Adapted from Ott (2009, 256).

Type of Field	*C*	*N*	*M*
Electric field	322	3	2
Plane wave	168	1	0
Magnetic field	14.6	-1	-2

This general equation covers the reflection loss to plane waves and in the near field. In the near field, the equation includes reflection loss associated with electric and magnetic fields. This expression does not account for the lessening in a material's shielding effectiveness from multiple reflections that occur in thin shields (Ott 2009).

In the case of graphene, the thickness is extremely thin. As previously indicated, the multiple reflection factor, B, can be omitted if the absorption loss, A, is higher than 9 dB, which is the case for multiple layers of graphene (Ott 2009). The multiple reflections factor can also be ignored for both the far field and near (electric) fields. Factor B contributes to the evaluation of Eq. (15) during near (magnetic) field situations as

$$B = 20\log\left(1 - e^{-2t/\delta}\right), \tag{18}$$

where δ is the skin depth (Ott 2009).

The thickness of the shield relative to the skin depth dictates how significantly the wave is attenuated as it propagates through the shielding material. The multiple reflections factor is less than zero, which signifies that less shielding is provided by thin materials due to the multiple reflections.

The skin depth is defined as the depth that the wave is attenuated to 1/e (37%) of its initial value. The skin depth is calculated by (Ott 2009)

$$\delta = \frac{2.6}{\sqrt{f\mu_r\sigma_r}} \text{ (inches)}. \tag{19}$$

6. Apertures

Apertures are openings in a shielding material that allow electromagnetic waves to penetrate into or out of an enclosure. Normal apertures are created during the manufacturing or assembly process of an electronic enclosure for mounting displays, indicators, and switches. Since graphene is structured on a 2D plane in the form of a hexagonal lattice formed by bonded carbon atoms, microscopically, it is not a solid thin film, which may significantly limit its shielding effectiveness when comparing it to commonly used shielding material (Ott 2009). To determine the shielding effectiveness of a single aperture, a quick assessment of its effect on a material's shielding effectiveness is (Ott 2009)

$$SE = 20\log\left[\frac{150}{fl}\right], \tag{20}$$

where

- f is the frequency (in MHz)
- l is the maximum linear dimension of an aperture (in m).

The maximum linear dimension of graphene's natural aperture is on the order of a couple of angstroms. Modeling graphene with openings of this size would give a shielding effectiveness greater than 150 dB at 1 GHz. Therefore, the aperture is considered negligible and graphene is evaluated as a solid thin film for concept design consideration.

III. CONCEPT DESIGN

A. CONCEPT GENERATION

With a preliminary list of product specifications available and a full dissection of the product conducted, a number of product concepts can begin to form (Dieter and Schmidt 2013, 38). A product concept is a unrefined idea constructed from current and evolving products and processes discovered from the information collected during dissection. A product concept can take many forms. A concept can range from a textual document to sketches and drawings. A product concept can also take the form of a simple, physical 3D model to a more defined computer generated one (Ulrich and Eppinger 2012).

Product development teams use several methods to generate product concepts. Dieter and Schmidt (2013) cite six of the favorably utilized ones.

- Functional Decomposition and Synthesis—decomposing the product into separate functions or actions without regard to physical components that may serve a function.

- Morphological Analysis—dividing the concept design into functionally based sub-problems for which a list of generic solutions is generated. Then the solutions are combined across sub-problems to form concepts.

- Theory of Inventive Problem Solving—better known by the Russian acronym, TRIZ, it is known for providing a design methodology specifically tailored for engineering and technical problems.

- Axiomatic Design—a method developed by Nam P. Suh to convert a distinct product behavior into functional requirements, which in turn, are used to develop design factors.

- Design Optimization—utilizing optimization algorithms to predict the best design from the established target specifications.

- Decision-Based Design (DBD)—this method differs slightly from others in that additional design outcomes related to how much profit can be generated and market shares gained will eventually determine the best concepts to move forward.

Ulrich and Eppinger (2012) use concept combination tables developed in the Morphological Analysis method. Concepts are generated using grouping fragments (solutions) from each sub-problem to construct a potential product that will hopefully address the customer's needs (Ulrich and Eppinger 2012). In practice, concept combination tables tend not to be as helpful when the number of sub-problems goes beyond three or four (Ulrich and Eppinger 2012). Table 7 is a concept combination table for generating concepts for producing a polymeric material fused with graphene.

Table 7. Concept Combination Table for Manufacturing a Lighter Weight EMI Shielding Material Utilizing Graphene. Adapted from Ulrich and Eppinger (2012, 134).

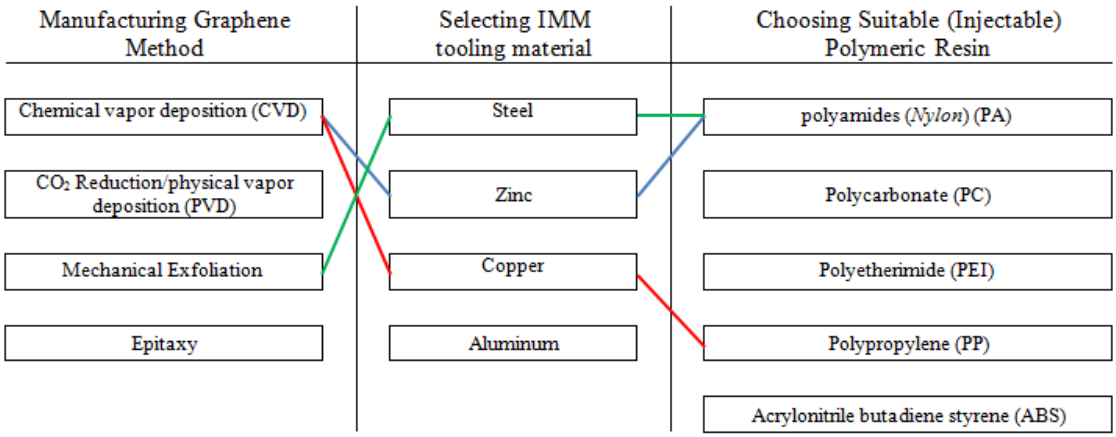

Concept 1—graphene developed via CVD on copper tooling and joined with a polypropylene resin

Concept 2—graphene developed via mechanical exfoliation placed on steel tooling and joined with a polyamide resin

Concept 3—graphene developed via CVD on zinc tooling and joined with a polyamide resin

B. CONCEPT SELECTION

After a number of viable concepts have been generated, concept selection begins an iterative process of evaluating the concepts against the target specifications and

customer needs (Urlich and Eppinger 2012). Figure 15 illustrates the repetitive process that occurs between concept generation and selection to narrow down the concepts to one (or a very few) that will proceed forward in the concept development phase of product development (Dieter and Schmidt 2013).

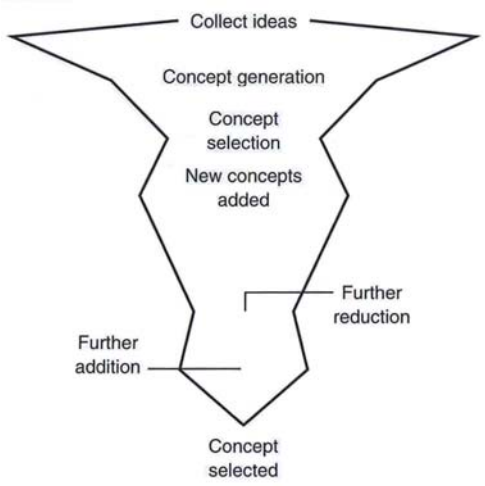

Figure 15. Concept Generation and Selection, Viewed as an Iterative Process. Source: Dieter and Schmidt (2013, 245).

Decision making is a problem-solving activity essential to select the best concept confidently. A decision strategy applicable to both the concept alternatives and the design phase of this portion of the product development process is needed to conduct the concept selection step successfully (Dieter and Schmidt 2013). To make a decision, the facts, the knowledge, and the experience surrounding the framework of the problem must be collected and evaluated. The facts, and thus the knowledge, have been collected from the previous product dissection. During this step, experience is needed to advise how the concepts generated vary or diverge from the current products and processes (Dieter and Schmidt 2013).

The practice of manufacturing electronic enclosures from plastic has been prevalent for reducing the weight of a product. To address the necessary shielding effectiveness required by the enclosure, a conductive coating can be applied to the walls of the enclosure, the plastic can be impregnated with a conductive filler when molded, or

both processes can be utilized (Ott 2009). However, those shielding practices provide only limited SE for particular frequency ranges. With the discovery of graphene (and related carbon nanotechnology), the customer hopes that graphene is the answer to providing plastics with a broader range of shielding capability (Moore 2011).

Thus, the emphasis of concept selection to address the need of this customer is not as focused on the product itself; but is more so, on the processes that deliver it. If the readiness of the technology needed to fabricate the product is not mature, then concept testing should not be started (Dieter and Schmidt 2013). When examining the components and processes used to manufacture the end product, the combined boundaries of the components must include the boundaries identified in the final product. This examination ensures that issues conceptualized for a graphene/plastic composite material have not been omitted (Langford 2012).

To evaluate the feasibility of adapting graphene manufacturing to the polymeric injection molding processes, the boundaries between the injection molding processes and graphene need to be established or defined. Langford stipulates that boundaries are defined by three different domains: physical, functional, and behavioral. The relationship between these boundaries is best illustrated in Figure 16.

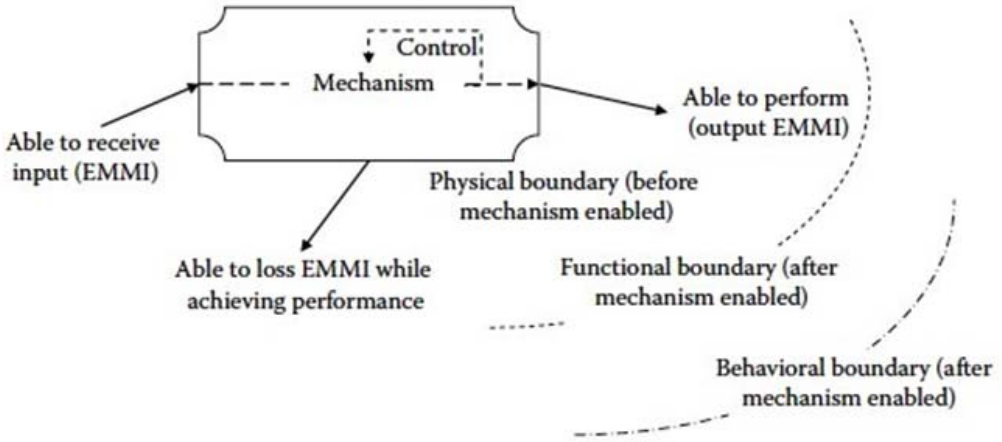

Figure 16. An Object's Boundaries Defined by an Object's Interaction with other Objects through Energy, Matter, Material Wealth, and Information (EMMI). Source: Langford (2012, 33).

The physical boundary of graphene would simply be the actual space that the graphene molecules occupy independent of "communication" with any other object. Functional boundaries have been identified between the graphene and the mold material at the beginning of the injection molding process and between graphene and the polymeric resin at the completion of the process. The functional boundaries exist due to the functional dependency of graphene to maintain its physical shape to ensure direct contact with the inner and outer physical boundaries of the mold and the molded plastic part. Many behavior boundaries are going from the manufacturing process of graphene to the intended end-use environment to which the molded part or parts are subjected. For the purposes of this investigation, however, the behavior boundaries of graphene are primarily focused on the IMM. The IMM has functional boundaries with the injection mold and molten resin; therefore, the IMM behaviorally affects the anticipation of the physical and functional boundaries between graphene, the mold, and the plastic resin (Langford 2012).

The success that the researchers from the University of Pennsylvania had with copper would bring attention to the use of beryllium-copper as a suitable substrate material that translates well to being employed as a tooling material for injection molding. The benefits identified would be that the beryllium-copper alloy can be polished for the desired surface finish and the graphene yield is highly single-layered and uniform. The main difference would be the thickness. The findings from the research conducted at the University of Pennsylvania were performed on copper foil. Tooling for injection molds is substantially thicker. The need to etch the copper away from the graphene when transferred to another substrate poses a problem.

If the thickness of the injection molding tooling is a parameter that would reduce the yield of producing a uniform, single-layer of graphene, then additional research is needed to investigate altering the steel tooling to accommodate a metal substrate that would stimulate graphene growth. The benefit of this approach is combining the choice material for graphene synthesis with the advantages associated with steel tooling. Heat treating the steel tooling to enrich the surface with another metal or material may be

limited. Altering the steel tooling to mate with another material would introduce new mechanical and thermal issues regarding the injection mold process.

CVD is a method used in both industries. The CVD process has been used to surface-treat steel tooling with carbides, metals, nitrides, borides, silicides, or oxide deposits. If the optimum metal can be utilized in the injection mold process, graphene can be manufactured directly on the tooling to eliminate the additional step of transferring graphene from one substrate to another. The main issue with the repetitive use of tooling is subjecting the tooling to the elevated temperatures of the CVD process. These temperatures greatly affect the hardness and strength of the material and potentially distort the features of the cavity.

The physical vapor deposition process used to coat injection mold tooling seems to coincide with the dry ice method of graphene development. Burning magnesium in a carbon dioxide environment conforms to the basics principles of the PVD technique, as shown in Figure 17. The benefit of the PVD process over the CVD process is that the operating temperatures are much lower, which eliminates the concern of distorting or affecting the heat treatment of the tooling. One issue is the introduction of contaminates, such as magnesium particles and the adhesion of the graphene.

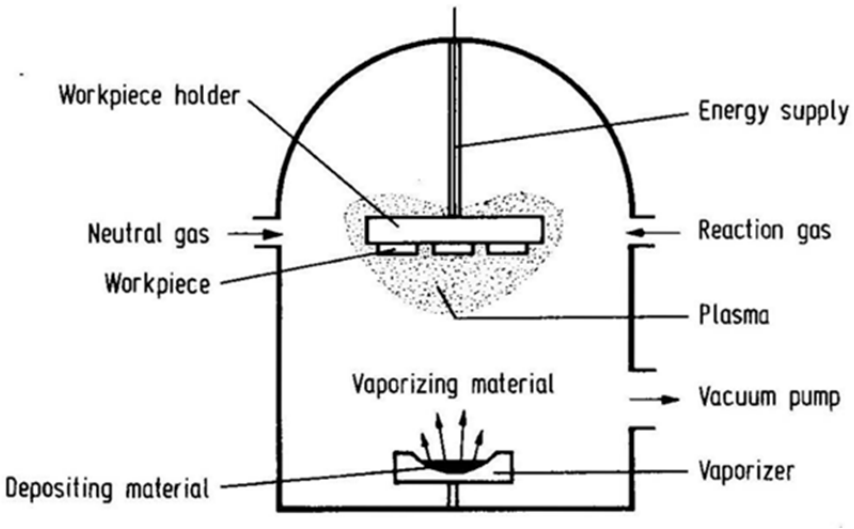

Figure 17. Basics of the PVD Technique.
Source: Menges and Mohren (1993, 26).

An alternative process is transferring graphene from its production site to the injection mold tooling. This process involves using the best material to synthesize the graphene and then including an additional process to transfer the nanostructure to the tooling. This process is beneficial because it guarantees the optimal solution for uniform, single-layer graphene generation. An additional step introduces a risk in the potential misapplication of the monolayer graphene on the mold. If the transfer process is not fully developed, it can greatly alter the electrical properties of the graphene by not maintaining a uniform, atomic layer across the entire surface of the mold. Additional processes can also affect quality and reliability during the transfer.

The mold or tooling material must be able to withstand the heat cycling and extreme pressures from repetitive part making. The final choice of material must balance the mechanical operations of the selected injection molding machine with the aesthetics of the finished product and cost factor to manufacture it. Not only can choosing the wrong material lead to poor quality of the end product but it can also result in increased life cycle costs of the injection mold process. Selection of the mold material must be able to provide excellent performance in service and to create the finished part with the desirable features and characteristics.

The sizing of the injection unit of the IMM is dependent on the amount of material it takes to shoot (create) one part. The ideal size, or capacity, of the heating cylinder, is twice the volume needed to fill the mold, which is considered one cycle. Therefore, preferably, the heating cylinder must be sized to be able to complete two cycles. In other words, 50% of the heating cylinder should be emptied each time the mold is filled. Some situations may arise that require operating the IMM injection unit away from this desired capability. If so, then the amount of heated plastic needed in one cycle of the injection mold must not be less than 20% or more than 80% of the heated resin within the heating cylinder. The heat sensitivity of the polymeric material factors greatly in determining the heating cylinder's volume when operating outside of the 50% rule of thumb.

The amount of molten resin needed for a single cycle of the mold also affects the amount of the clamping force needed to keep the mold halves shut until the polymeric

material has solidified. Table 8 shows the typical amount of clamping force needed for given amounts of injected plastic.

Table 8. Clamping Force for a Determined Amount of Molten Resin.
Source: Bryce (1996, 12).

Clamp size, tons (kilonewtons)	**Shot size, oz. (g)**
10 (89)	½ (14.2)
25 (222.5)	2 (56.7)
50 (445)	4 (113.4)
100 (890)	8 (226.8)
200 (1780)	16 (453.6)
250 (2225)	20 (567)
300 (2670)	30 (851)

The guidelines in Table 8 follow the general requirements that the clamping force needs to be in the range of two to eight times the projected area that is perpendicular to the hydraulic actuator and metering screw of the IMM and an additional 10% increase with every inch over a 1-inch depth of the molded part. This additional IMM requirement is also dependent upon the fluid flow characteristics of the polymeric material being injected. The injection pressure is determined by the viscosity of the molten material, which leads to the design requirements of the metering screw and nozzle. These additional stipulations must come back and comply with the actual volume of material needed to mold the part and the volume requirements of the heating cylinder.

IV. CONCEPT REFINEMENT

A. CONCEPT TESTING

The current DOD standard for electromagnetic compatibility (EMC) limitations is MIL-STD-461G. This standard specifies conducted and radiated limits for emission and susceptibility of military and aerospace products in the frequency range of 30 Hz to 40 GHz. Unlike the standards used in the commercial sector, this standard is typically more stringent than the standards of the Federal Communications Commission (FCC) and is not legally required. The requirements of MIL-STD-461G are contractual based. Under the domain of DOD contracts, EMC limits called out for products can be negotiated (i.e., reduced range of frequencies, lower level of shielding effectiveness that is acceptable, or a change in the distance from which measurements are recorded) or in rare cases, waived. In addition, the EMC specifications are application dependent with different limits for different operational environments (Ott 2009). Table 9 lists the frequency ranges for the radiated emission and susceptibility requirements specified.

Table 9. Frequency Ranges for Radiated Emission and Susceptibility Requirements in MIL-STD-461G. Adapted from U.S. Department of Defense (2015, 25).

Requirement	Description
RE101	Radiated Emissions, Magnetic Field, 30 Hz to 100 kHz
RE102	Radiated Emissions, Electric Field, 10 kHz to 18 GHz
RE103	Radiated Emissions, Antenna Spurious and Harmonic Outputs, 10 kHz to 40 GHz
RS101	Radiated Susceptibility, Magnetic Field, 30 Hz to 100 kHz
RS103	Radiated Susceptibility, Electric Field, 10 kHz to 40 GHz
RS105	Radiated Susceptibility, Transient Electromagnetic Field

Based on all the radiated emission and susceptibility requirements listed in MIL-STD-461G, an electronic enclosure can be evaluated over a very large range of frequencies while assessing its shielding effectiveness in both near and far field conditions. Selecting a material of a specific thickness for an enclosure to meet all the radiated requirements is challenging with conventional shielding material. To narrow the

focus of considering graphene as an option, Table 10 lists the general applicability of those shielding requirements for appropriate military environments.

Table 10. Requirement Applicability Matrix for Radiated Emission and Susceptibility in MIL-STD-461G. Adapted from U.S. Department of Defense (2015, 26).

Equipment Installed In, On, or Launched From the Following Platforms or Installations	**RE101**	**RE102**	**RE103**	**RS101**	**RS103**	**RS105**
Surface Ships	A	A	L	A	A	L
Submarines	A	A	L	A	A	L
Aircraft, Army, and Flight Line	A	A	L	A	A	L
Aircraft, Navy	L	A	L	L	A	L
Aircraft, Air Force	N	A	L	N	A	N
Space Systems and Launch Equipment	N	A	L	N	A	N
Ground, Army	N	A	L	L	A	N
Ground, Navy	N	A	L	A	A	L
Ground, Air Force	N	A	L	N	A	N

A = applicable, L = limited applicability as specified in the standard, N = not applicable.

To determine if a graphene impregnated polymeric enclosure can be an alternative for the customer, a set of benchmarks is needed to evaluate the SE of graphene for a given frequency and field conditions. Table 11 proposes the attenuation levels for judging the suitability of graphene. The test equipment utilized in EMC certification has a maximum dynamic range of around 100 dB. For this reason, if any SE value is higher than 90 dB, the material is considered impenetrable (LearnEMC).

Table 11. Qualitative Benchmark for Shielding Effectiveness. Adapted from Ott (2009, 298).

Key	**Attenuation**
Bad	0–10 dB
Poor	10–30 dB
Average	30–60 dB
Good	60–90 dB
Excellent	> 90 dB

The evaluation of graphene's SE begins with RE102 and RS103 since these requirements are applicable for all military operational environments. The requirements for RE102 from MIL-STD-461G are to verify that the radiated electric field emissions from the product do not exceed the stipulated limits. The radiated field is measured at a distance of 1 m from the test setup boundary. The requirements for specific military operational environments are as follows (U.S. Department of Defense 2015).

- Ground 2 MHz to 18 GHz
- Ships, Surface 10 kHz to 18 GHz
- Submarines 10 kHz to 18 GHz
- Aircraft (Army and Navy) 10 kHz to 18 GHz
- Aircraft (Air Force) 2 MHz to 18 GHz
- Space 10 kHz to 18 GHz

RS103 looks at an enclosure's ability to prevent the product from being infiltrated by external EMI. The requirements of RS103 are to test a product's ability to operate as intended without failure or reduction in its ability to function under design operational conditions when subjected to the radiated electric fields listed as follows. The radiated source is located at a distance of 1 m or more (U.S. Department of Defense 2015).

- Army, Navy and optional* for all others 2 MHz to 30 MHz
- All 30 MHz to 18 GHz
- Optional* for all 18 GHz to 40 GHz

*Required only if specified in the procurement specification.

Although radiated emissions are comprised of both electric and magnetic fields, RE102 and RS103 only require that the electric fields be measured for compliance.

1. Modeling Intrinsic Graphene

Two models of a polymeric enclosure with graphene will be developed. One model will be a plastic enclosure with a single layer of graphene bonded to the interior wall. The other model will be the same enclosure with two, single layers of graphene; one on the interior wall and one on the exterior. Figure 18 displays the 3D models of an injection molded part with simulated graphene fused with the molded resin.

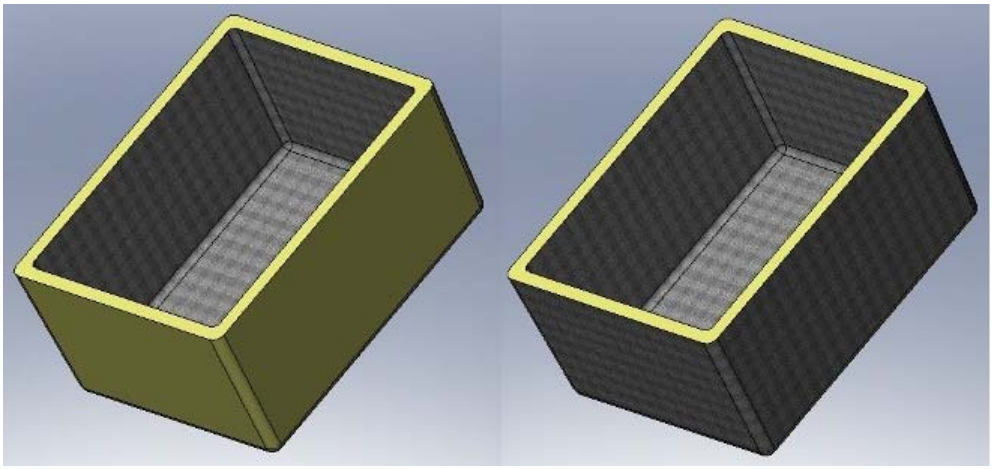

Figure 18. Polymeric Enclosures with a Single Layer of Graphene (Left) and (2) Single Layers (Right).

Electrical characteristics aside, the ability of an enclosure's material to shield electromagnetic frequencies is the same whether it is being evaluated for reducing the emissions of internal electronics or preventing the penetration of outside electromagnetic noise. The distance from the source also determines if a particular material is effective (Ott 2009, 238). For RE102, the polymeric/graphene material will be very close to the source (within centimeters or inches), as it serves to prevent the release electromagnetic emissions to the environment from the internal electronics; thus, the material will be placed in a predominately near, electric field environment.

In the case of RS103, the radiated source will be placed 1 m from the enclosure. The higher the frequency emanating from a predominately electric field source, the shorter the distance the transition region is from the radiating source. At any point

beyond that distance, the wave impedance will be equal to the impedance of air, and therefore, the shielding effectiveness of a material can be analyzed for plane waves (Ott 2009). The wavelength of a radiated source with a transition region of 1 m can be defined by (Ott 2009)

$$1 = \frac{\lambda}{2\pi} \text{ or } \lambda = 2\pi \,. \tag{21}$$

For this transition region, the wavelength will be ≈ 6.28 m. The wavelength's associated frequency is determined by (Clayton 2006)

$$f = \frac{c}{\lambda} \,. \tag{22}$$

The velocity of an electromagnetic wave traveling through air is given as (Clayton 2006)

$$c = 3 \times 10^8 \text{ m/s.} \tag{23}$$

Thus, the frequency of a wave with a transition region of 1 m is approximately 47.77 MHz (which is roughly 50 MHz). At this point, frequencies higher than 50 MHz have entered or exited their transition region and exhibited characteristics of a plane wave at the distance of 1 m. As a result, the modeling of graphene's shielding effectiveness for frequencies greater than 50 MHz can be examined in a far field (plane wave) condition.

a. RS103—Plane Wave

(1) Conductivity Analysis.

The RS103 test measures the radiated emissions from a product to determine if those emissions are within the limits stipulated for a given frequency range. In this situation, graphene is shielding the internal electronics from external radiated source 1 m away. Applying the plane wave constants from Table 6 to Eq. (16), (17), and (18), the overall shielding effectiveness of graphene can be calculated in a plane wave environment. Table 12 exhibits the calculated SE of intrinsic graphene to plane waves for frequencies from 50 MHz to 18 GHz using the volume conductivity of graphene in Table 4.

Table 12. Single Layer of Intrinsic Graphene—Calculated Shielding Effectiveness for Plane Wave of Frequencies Greater than 50 MHz

Frequency	Location of Transition Region (cm)	Absorption Loss (dB)	Reflection Loss (dB)	Multiple Reflections (dB)	Total SE
50 MHz	95.5	0.000406145	93.289	-80.581	12.709
110 MHz	43.4	0.00060241	89.865	-77.157	12.709
210 MHz	22.7	0.000832349	87.057	-74.349	12.709
310 MHz	15.4	0.001011292	85.365	-72.657	12.709
410 MHz	11.7	0.001163021	84.151	-71.443	12.709
510 MHz	9.4	0.001297122	83.203	-70.495	12.709
1.04 GHz	4.6	0.001852304	80.109	-67.401	12.709
2.04 GHz	2.3	0.002594243	77.183	-64.476	12.709
3.04 GHz	1.6	0.003166886	75.450	-62.744	12.709
4.09 GHz	1.2	0.003673307	74.162	-61.456	12.709
5.09 GHz	0.9	0.004097835	73.212	-60.507	12.709
9.99 GHz	0.5	0.005740879	70.283	-57.580	12.709
15.09 GHz	0.3	0.007055702	68.492	-55.790	12.709
18.09 GHz	0.3	0.007725292	67.704	-55.003	12.709

From the data in Table 12, it appears that intrinsic graphene provides an overall SE of approximately 13 dB at frequencies greater than 50 MHz. At that value, the overall shielding effectiveness of graphene is considered poor. However, the factors that contribute to the overall shielding effectiveness give more insight into the regions where graphene may be applicable. With the absorption loss being directly proportional to a material's thickness, it is clear that the portion of the overall shielding effectiveness is essentially zero for this range of frequencies. At graphene's thickness, graphene would not show appreciable absorption loss (> 5 dB) until well past 7,000 Terahertz (THz). The portion of the overall shielding effectiveness associated with the reflection loss is particularly high due to the intrinsic nature of graphene's very high conductivity and relatively low permeability. However, due to the multiple reflections innate to thin film materials, the overall shielding effectiveness is substantially reduced.

(2) Sheet Resistance Analysis

In the realm of thin films, graphene is extremely thin. In the evaluation of semiconductor wafers, a four-point probe is used to measure the wafer's resistivity (Schroder 2006). Depending on the thickness of the sample, the distance between each

probe typically ranges from 0.5 to 1.5 mm (7). Once the thickness, or thinness in this case, of a thin film, is equal to or less than half the value of the probe spacing, a thin film's resistance becomes categorized as sheet resistance, R_{sh}. The relationship of sheet resistance to a material's conductivity (σ), resistivity (ρ), and the thickness (t) is expressed as (9) (Schroder 2006)

$$R_{sh} = \frac{1}{\sigma t} = \frac{\rho}{t}. \tag{24}$$

To understand the idea of sheet resistance better, Figure 19 shows a material of the resistance between the two nodes as (Schroder 2006),

$$R = \rho \frac{L}{A} = \rho \frac{L}{Wt} = \frac{\rho}{t}\frac{L}{W}\ \Omega. \tag{25}$$

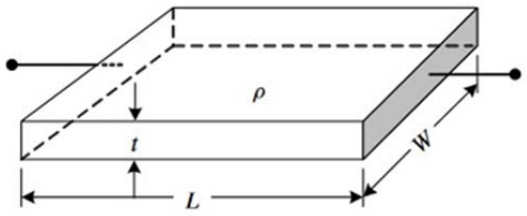

Figure 19. Concept of Sheet Resistance. Source: Schroder (2006, 11).

Since L/W is unitless, the value of ρ/t will maintain the units of Ohms, but its value is not the same as the resistance (R) associated with a material's bulk properties. To differentiate between R and ρ/t, the ρ/t relationship, R_{sh}, takes on the units of Ω/square or Ω/□. So, the relationship between a material's bulk resistance and sheet resistance can be expressed as (Schroder 2006)

$$R = R_{sh}\frac{L}{W}\ \Omega. \tag{26}$$

Applying Eq. (24) with the volume conductivity ($\sigma = 10^8$ S/m) and thickness of intrinsic graphene ($t = 3.36\times10^{-10}$ m) yields a sheet resistance value of 29.76 Ω/□. This value is close to the 30 Ω/□ reported in research conducted by Chen et al. (2008).

CST STUDIO SUITE® 2015 is simulation software used to design and simulate electronics for improving electromagnetic considerations. It was used to model and simulate the shielding effectiveness of a single layer of graphene bonded to a polymeric material by utilizing the sheet resistance parameter. Figure 20 provides a 3D view of the model with a single layer of graphene bonded to the interior wall shown in Figure 18.

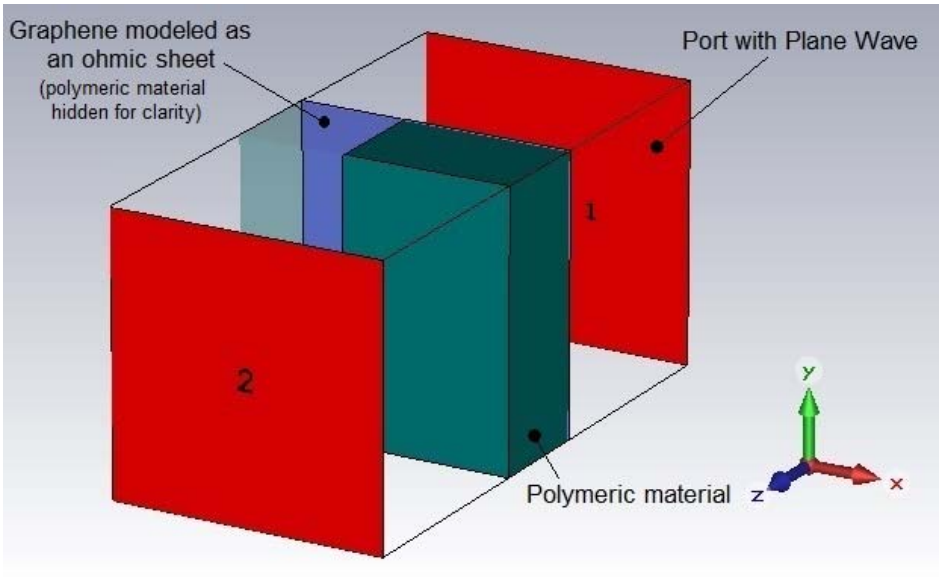

Figure 20. CST STUDIO SUITE Model of a Single Layer of Graphene Bonded to a Polymeric Material

The polymeric material was modeled with a thickness of 4 mm with a relative permittivity of 3 and a conductivity of 10^{-11} S/m. The graphene sheet was modeled as an ohmic sheet with a sheet resistance of 30 Ω/□. The polymeric/graphene model's boundaries in the X and Y axis were extended infinitely. The area between the Port planes was defined as free space or air. Port 1 was set up to provide the default Gaussian excitation signal with a polarization angle of 0° (See Figure 21). Port 2 was set up to record the transmission loss through the polymeric/graphene model.

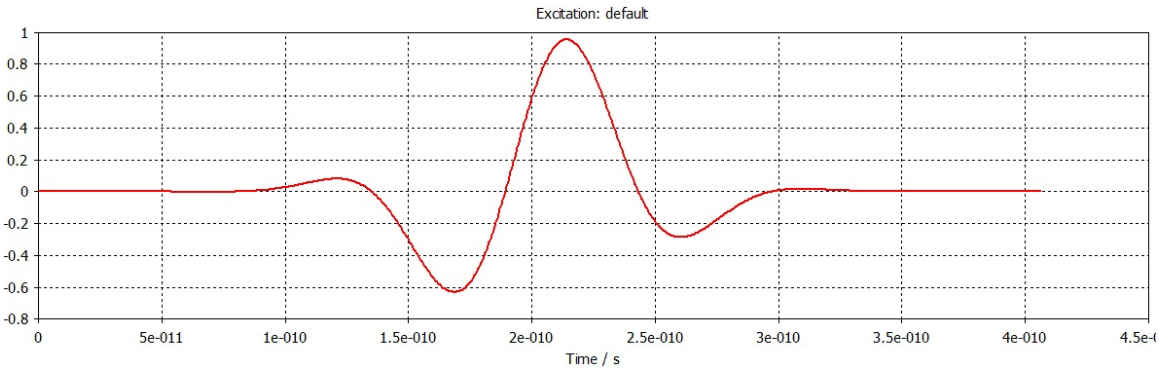

Figure 21. Default Excitation Signal from Port 1

The resulting shielding effectiveness, shown in Figure 22, varied between 13.6 dB to 17.2 dB across the frequency range of 50 MHz to 18 GHz.

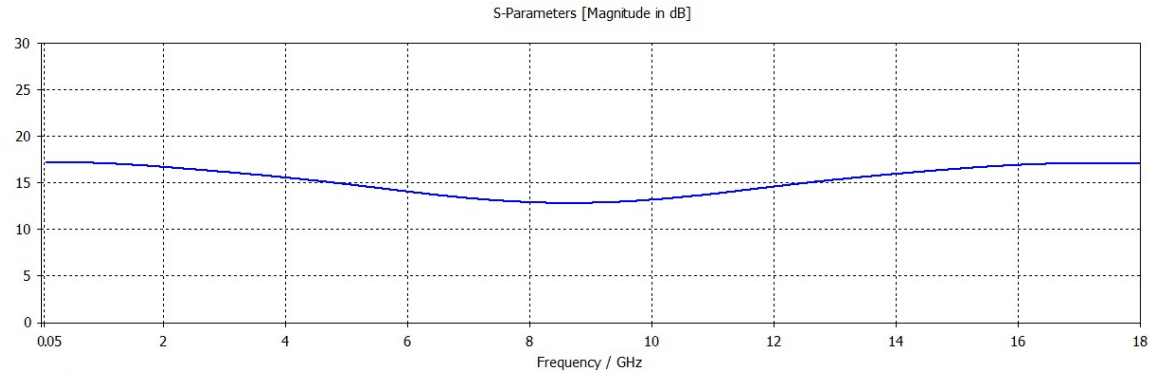

Figure 22. Single Layer of Intrinsic Graphene—Modeling and Simulation of Shielding Effectiveness for Plane Wave of Frequencies 50 MHz to 18 GHz

The simulation results from modeling graphene as an ohmic sheet within +0.9 dB to +4.5 dB of the calculated values using graphene's conductivity. The data from the simulation indicates graphene to be a poor choice for shielding effectiveness for this range of frequencies, given that values greater than 50 dB are desired.

To compensate for the poor performance of a single layer of graphene, a polymeric enclosure may be molded with two layers of graphene as shown in Figure 18; one internally and one externally. For this scenario, CST STUDIO SUITE® was used

again, but this time to model and simulate the shielding effectiveness of two, single layers of graphene bonded to a polymeric material as represented in Figure 23.

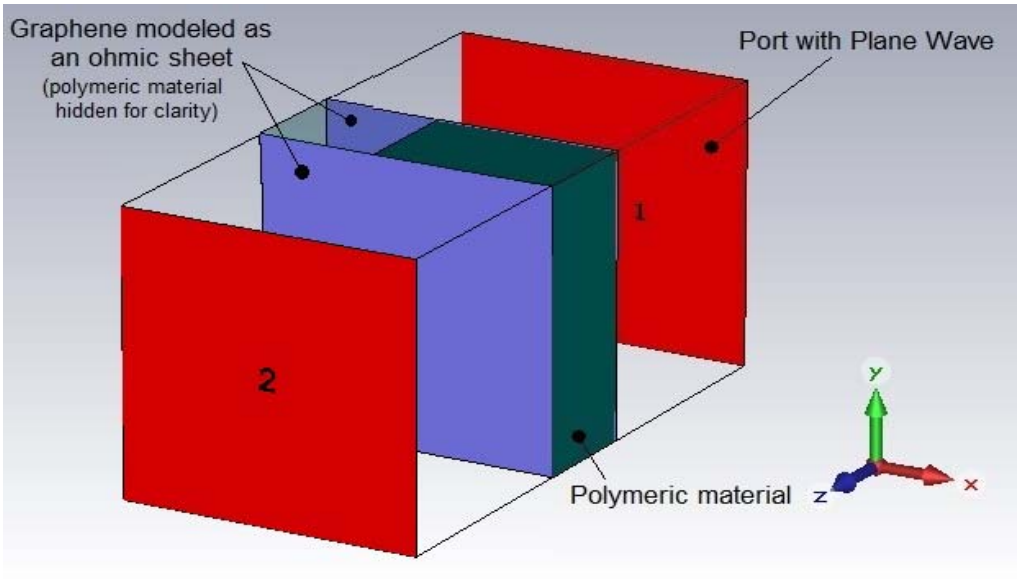

Figure 23. CST STUDIO SUITE Model of Two, Single Layers of Graphene Bonded to a Polymeric Material

The sheet resistance parameter was retained to define the electrical property of both, individual layers. The results of the analysis are shown in Figure 24. With the extra layer of graphene, the shielding effectiveness of the polymeric/graphene material doubled to vary between 25.3 dB to 34.5 dB across the same frequency range of 50 MHz to 18 GHz. With the extra layer of graphene, the overall shielding effectiveness of the combined material moves up the qualitative poor range and begins to enter the average benchmark.

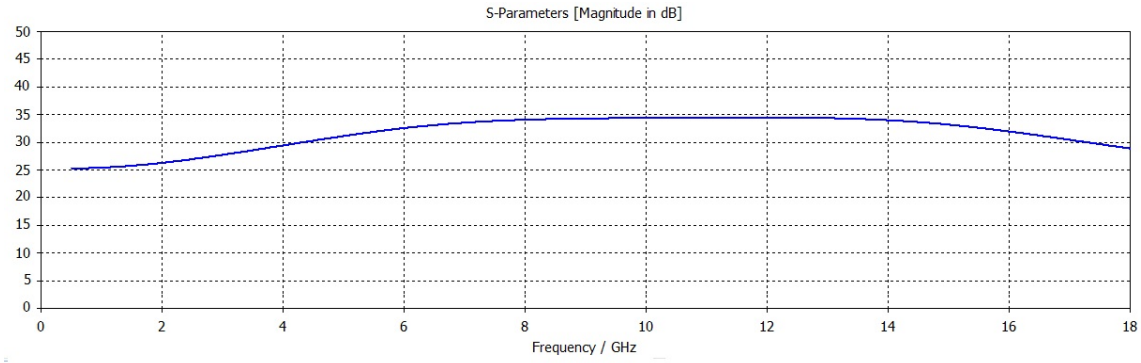

Figure 24. Two, Single Layers of Intrinsic Graphene—Modeling and Simulation of Shielding Effectiveness for Plane Wave of Frequencies 50 MHz to 18 GHz

b. RE102—Electric Field

The RE102 test measures the radiated emissions from a product to determine if those emissions are within limits stipulated for a given frequency range. In this situation, graphene is shielding internal electronics and is relatively close to the radiated sources. Applying the near, electric field constants from Table 6 to Eq. (16), (17), and (18), the overall shielding effectiveness of graphene can be calculated in a near, electric field environment. Table 13 displays the calculated SE of intrinsic graphene to near, electric field waves at 5 centimeters (cm) for frequencies from 10 kHz to 510 MHz.

Table 13. Single Layer of Intrinsic Graphene—Calculated Shielding Effectiveness for Near, Electric Field for Frequencies from 10 kHz to 510 MHz at 5 cm from Source

Frequency	Location of Transition Region	Absorption Loss (dB)	Reflection Loss (dB)	Multiple Reflections (dB)	Total SE
10 kHz	4,777 m	5.74375E-06	178.258	-117.570	60.688
50 kHz	955 m	1.28434E-05	157.289	-110.580	46.709
100 kHz	477 m	1.81633E-05	148.258	-107.570	40.688
500 kHz	95.5 m	4.06145E-05	127.289	-100.580	26.709
1 MHz	47.8 m	5.74375E-05	118.258	-97.570	20.688
5 MHz	9.6 m	0.000128434	97.289	-90.580	6.709
10 MHz	4.8 m	0.000181633	88.258	-87.570	0.688
50 MHz	95.5 cm	0.000406145	67.289	-80.581	0
110 MHz	43.4 cm	0.00060241	57.016	-77.157	0
510 MHz	9.4 cm	0.001297122	37.031	-70.495	0

Based on the results, the overall shielding effectiveness is considered poor for frequencies 10 kHz to 1 GHz at the 5-cm distance. Graphene provides no SE from 50 MHz to 510 MHz whose transition regions extend beyond the established 5-cm distance. All frequencies above 1 GHz up to 18 GHz from a 5 cm distance are in plane wave condition. To increase the shielding effectiveness for radiated emissions, a polymeric/ graphene enclosure needs to increase in size to provide greater distance from internal, radiated sources so that more frequencies below 1 GHz can enter into a plane wave state before striking the material.

2. Modeling Extrinsic Graphene

Since an injected molded model does not provide substantial SE, an alternate approach is to model graphene as an enclosure material built with a layering resin to allow the use of multiple layers of graphene. Knowing that graphene's conductivity decreases when bonded to a substrate, multiple layers are needed potentially to provide any substantial SE. The first parameter that needs to be determined is the conductivity of graphene that generates a SE value of zero. By applying the plane wave constants from Table 6 to Eq. (17) and (18), setting the equations equal to each other, and solving for σ_r, results in a relative conductivity for an extrinsic graphene of 0.39124, which relates to an extrinsic conductivity of approximately 2.3×10^7 S/m. This value is slightly below the conductivity for aluminum. Graphene bonded to a substrate that limits its conductivity to this value or lower does not provide any measurable SE for plane wave frequencies of 50 MHz to 18 GHz.

As the model of the two, single layers of graphene constructed in CST STUDIO SUITE® revealed, the shielding effectiveness simply doubled that of a single layer. Based on that assumption, the number of layers needed to achieve a particular SE can be calculated from various estimates of conductivity for extrinsic graphene. Table 14 displays the number of layers of graphene needed to provide SE for a given dB level.

Table 14. Graphene Layers Needed to Achieve Desired Shielding Effectiveness

Conductivity	Layers of Graphene needed for Given SE For Plane Wave greater than 50 MHz			
	10 dB	**30dB**	**60dB**	**90dB**
Equivalent to Al	> 2	> 7	> 14	> 21
Equivalent to Au	> 1	> 5	> 10	> 15
Equivalent to Cu	> 1	> 3	> 7	>11
Equivalent to Ag	> 1	> 3	> 6	> 10

B. SETTING FINAL SPECIFICATIONS

The outcome of concept testing provides an organization with the ensuing design to permit the reexamination of the target specifications. Specifications can be enhanced from the broad range and targets established earlier in the Concept Development phase of product development (Urlich and Eppinger 2012).

However, in some cases, concept testing can also lead to the conclusion that a viable option other than the ones that currently exist may not be possible. With the insertion of utilizing a multilayer graphene material, the wrong concept (injection moldable) may have been chosen. DOD's attempt to bridge the gap between metal enclosures and conductive filled/coated plastic enclosures by utilizing graphene as a broad solution does not appear to be available at this point. An injection molded enclosure's process can render it to be suitable for bonding only two layers, one internally and one externally. Based on the analysis, it is not cost effective to produce an enclosure with this method because its intrinsic SE of nearly 35 dB is reduced to slightly greater than 10 dB when bonded to a polymeric material.

If the customer expressed interest in the multi-layer graphene option, the product development process would reenter the Concept Development phase at the concept generation step. The process would be repeated for the new idea.

THIS PAGE INTENTIONALLY LEFT BLANK

V. SUMMARY AND CONCLUSIONS

Graphene as a single layer does not provide any significant absorption loss contributions to the overall SE in plane wave or near field conditions for the frequencies covered in MIL-STD-461G. Figure 25 exhibits the total shielding effectiveness, along with the components, of a monolayer (intrinsic) graphene in plane waves.

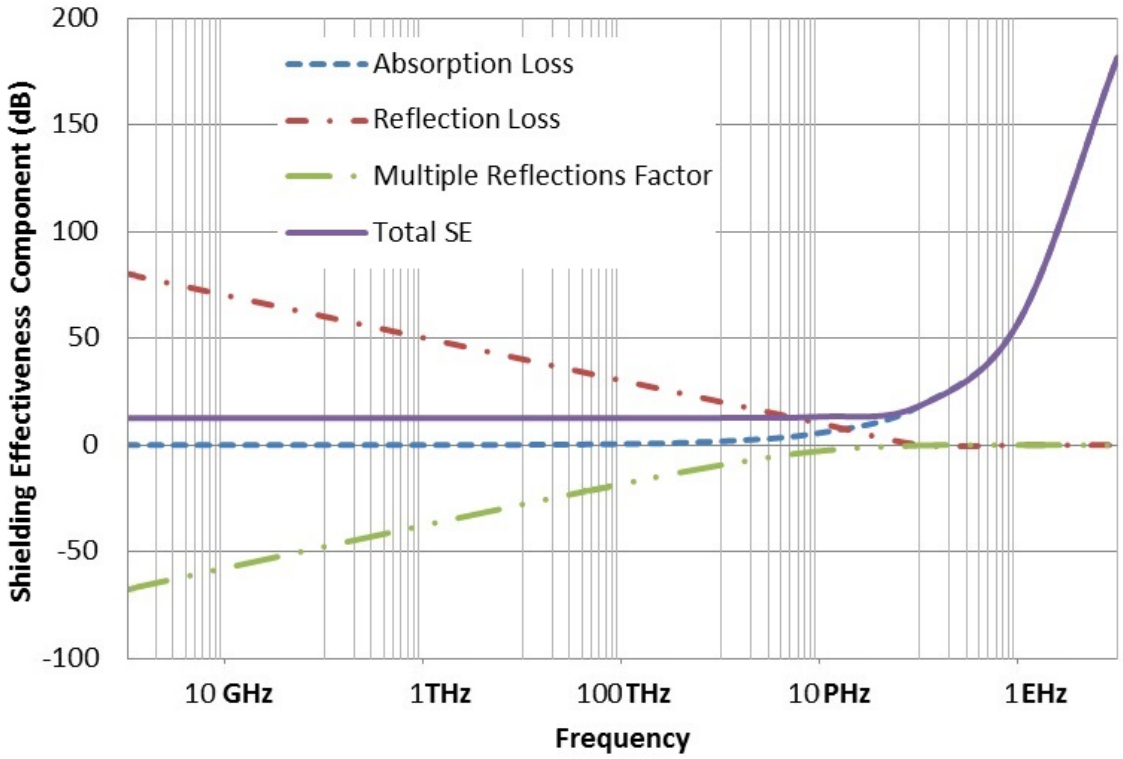

Figure 25. Shielding Effectiveness of Monolayer (Intrinsic) Graphene in the Far Field

Theoretically, the model of a single layer of intrinsic graphene in Figure 25 shows that it does not provide any appreciable shielding effectiveness until well into the ionizing radiation class (X-rays and Gamma rays) of the electromagnetic spectrum, which is well beyond the scope of military applications. Graphene bonded to a substrate

generally lowers the SE at each frequency. However, adding multiple layers does increase the SE, which can be an option if weight is an issue but volume is not.

Providing no absorption loss and having a relative permeability of one, it also becomes very evident that graphene does not provide any shielding effectiveness for near, magnetic field conditions. In the event that a government office issued a request for proposal (RFP) that stipulates RE101 and RS101 (radiated emissions and susceptibility to magnetic fields) as contractual requirements on the product offering, graphene (if an option) would not be part of the contractor's packaging solutions. Not even a multi-layer option provides magnetic field shielding.

Monolayer graphene does exhibit an exceptional amount of reflection loss in near, electric field conditions. However, multiple reflections due to the extraordinary thinness counter the benefit. With the knowledge that a substrate's conductivity decreases (or sheet resistance increases) when bonded to graphene, it becomes more challenging to leverage the SE created from graphene's reflection loss. In the interest of developing a multi-layer graphene composite, if the bonded polymeric material reduced the conductivity of graphene below 2.3×10^{7} S/m, the resultant composite material does not provide any SE for the frequencies required in MIL-STD-461G regardless of the number of layers used.

Seemingly, DOD's expectation was for intrinsic graphene to provide considerable shielding effectiveness to warrant the cost that would be associated with constructing an enclosure with such material. Since its discovery, the focus on graphene's incredible conductivity value has driven the research to explore all its possible uses. In the realm of electromagnetic shielding, graphene's thickness becomes its limiting factor. Common shielding metals maintain a bulk conductivity value that can be fabricated with various thicknesses. Graphene, on the other hand, has a specific conductivity for a finite thickness. The thickness renders graphene impractical as a shielding material in most cases.

A. PRODUCT PLANNING AND ANALYSIS

If the results of another round of concept generation, selection, and testing of the multilayer graphene option lead to maturing the final specifications, those specifications may flow down to begin development of technical models. Decision making and trade-off exercises can prepare the concept for the next phase of product development, system-level design. Staffing and budget requisites begin to develop for preparing forthcoming contracts. Economic models are generated to determine financial feasibility of the product. The initial steps to developing cost models begin with building competitive maps. Competitive costing maps can be constructed to address manufacturing cost, material cost, and forecasting sales to define trade-off curves from which to support the decision-making process (Urlich and Eppinger 2012).

As for the scenario covered in this document, if the customer can identify a specific instance or product that currently complies with stipulated EMI requirements but needs to be manufactured lighter, that particular product must enter the product development process. The internal electronics can be evaluated to determine the EMI source(s). Once the major sources have been identified, then on a smaller scale, an injectable molded graphene shield solution can be applied at a local level to reduce the demands on the overall enclosure. Modeling and simulation provide a litmus test to ascertain if the internal emissions have been reduced; thereby, providing opportunities to redesign the exterior enclosure akin to reducing enclosure thickness or changing the material.

B. POTENTIAL FUTURE WORK

With the exception of the injection molding process, future work goes well beyond investigating graphene for EMI shielding. Maturing the production of graphene is a necessity. Universities, private companies, and government research laboratories are continuing to explore ways to mass produce graphene. Currently, graphene is only produced in samples ranging from 1 square inch to a 4-inch diameter.

A number of other commercial uses will mature graphene production. One of the leading commercial uses for graphene is optoelectronics, for items, such as photovoltaic

cells and touch screens. This application alone can mature graphene's production. Ultrafiltration is another example. Although water can flow freely through graphene, it is essentially impermeable to particles as small as 5 nm. If the application of synthesizing graphene with an injectable molded resin is not useful for EMI suppression, a polymeric/ graphene composite material may be very tough, firm, and light. A material of this type can replace some instances of steel regarding environmental conditions of shock and vibration (Graphenea 2017).

In regards to EMI shielding, the concept of manufacturing a composite material comprised of multiple, single layers of graphene can provide substantial shielding effectiveness. That effectiveness depends on the number of graphene layers, distance from the source, and the resulting conductivity graphene possesses when bonded to a particular polymer, such as one more suited to being built with a layering technique. An injection-moldable polymer does not support the production of multilayer graphene composite.

The exploration of using graphene for EMI shielding purposes is ongoing. A study was conducted that showed the carrier density of graphene could be changed by chemical doping. As the chemical potential was increased, the conductivity increased but was only observed for a specific range of frequencies (Hanson 2008). Research has been performed to show an increase in the shielding effectiveness of graphene if placed in an electrostatic and magnetostatic bias. During this investigation, Lovat modeled graphene as an anisotropic material. In Figure 26, the shielding effectiveness of a monolayer graphene was more than doubled when a 5 V/nm electrostatic bias was applied (Lovat 2012).

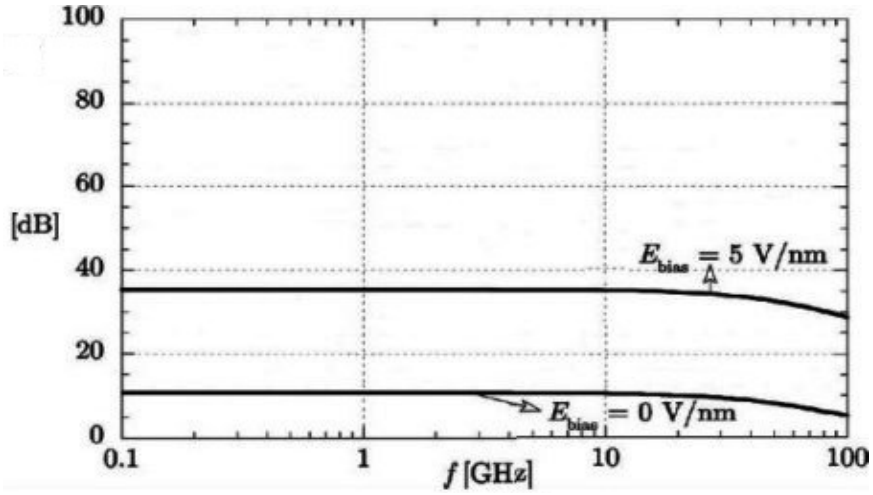

Figure 26. Shielding Effectiveness as a Function of Frequency for Unbiased and Electrostatically-biased Graphene. Adapted from Lovat (2012, 107).

Both these approaches introduce additional integration concerns, of course. Integrating an electrical or chemical bias into an enclosure increases complexity, this, in turn, increases cost. Also, the grounding of components and circuit boards must be redesigned.

In the meantime, the focus should be placed on individual components and sub-assemblies when packaging electronics. On a small scale, a polymeric/graphene material may be used to isolate near, electric fields emanating internally from components to help the outer enclosure's ability to satisfy MIL-STD-461G EMI requirements. This approach assists in lightening the enclosure of military electronics, as well as accelerates the learning curve for graphene and its uses.

THIS PAGE INTENTIONALLY LEFT BLANK

APPENDIX A. HALL COEFFICIENT FOR SELECTED METALS AND ALLOYS

The carrier density of a metal or metal alloy can be obtained by knowing the Hall coefficient of that particular metal. With the assumption that the conductivity of most metals is due solely to free electrons, the expression for the Hall coefficient, R_H, can be simplified as

$$R_H = -\frac{1}{n_e e}. \tag{27}$$

The greater the carrier concentration within a metal, the lower the magnitude of the material's Hall coefficient. The expression for a material's Hall coefficient becomes more complex if both electrons and holes influence the conductivity (Kittel 2005).

For most nearly free electron metals, the Hall coefficient will be a negative number. However, for some metals that fall into this category, the Hall coefficient can be a positive number as the electron(s) move from its current energy band to a higher energy band, which creates a "hole" in the previous energy band (Kittel 2005). Table 15 lists experimental values of R_H for selected metals and metal alloys. All the data collected from experimentation was conducted on the solid-state phase of the metal.

Table 15. Experimental Hall Coefficients of Selected Metals and Alloys. Adapted from Hurd (1972, ch. 7).

Material	Composition		Base Material	Temperature of Measurement	Hall Coefficient (10^{-11} $m^3/A \cdot s$)
Silver (Ag)	Pure element		Ag	293 K	-8.97 (pg 220)
Gold (Au)	Pure element		Au	RT (room temperature)	-7.36 (pg 242)
Aluminum (Al)	Pure element		Al	287.6 K	-3.44 (pg 232)
Nickel (Ni)	Pure element		Ni	RT	-0.607 (pg 332)
Iron (Fe)	Pure element		Fe	RT	0.97 (pg 292)
Carbon Steel (1018)	Carbon, C	0.14–0.20%	Fe + 1.18 wt. % C (as received)	293 K	1.55 (pg 257)
	Iron, Fe	98.81–99.26%	See Iron (Fe)		
	Manganese, Mn	0.60–0.90%	Fe + 3.4 % Mn	RT	3.15 (pg 296)
	Phosphorus, P	≤ 0.040%			
	Sulfur, S	≤ 0.050%			
Stainless Steel (304)	Carbon, C	≤ 0.080%			
	Manganese, Mn	≤ 2.00%	Fe + 3.4 % Mn	RT	3.15 (pg 296)
	Silicon, Si	≤ 0.75%			
	Phosphorus, P	≤ 0.045%			
	Sulfur, S	≤ 0.030%			
	Chromium, Cr	18.00–20.00%	Fe + 5.98 % Cr	RT	4.63 (pg 273)
	Nickel, Ni	8.00–12.00%	Data unavailable for Fe-Ni at this percentage		
	Nitrogen, N	≤ 0.010%			
	Iron, Fe	≥ 65.085	See Iron (Fe)		

The values recorded in Table 15 for the Hall coefficient of metals with magnetization characteristics are composed of an ordinary Hall coefficient, R_0, and the addition of a spontaneous Hall coefficient, R_8. In temperatures where the metal is in a ferromagnetic state, R_8, is found to have a strong influence on the overall Hall coefficient based on the temperature; whereas, R_0 is temperature independent. Therefore, the Hall coefficient of magnetic metals (i.e., Ni, Fe, Fe+C) is called the extraordinary Hall coefficient, R_1, and is expressed as the quantity of $4\pi(R_0 + R_8)$ (Hurd 1972).

THIS PAGE INTENTIONALLY LEFT BLANK

APPENDIX B. ARRANGEMENT OF ELECTRONS AROUND THE NUCLEUS

First, electrons in the electron cloud that surrounds the nucleus of an atom are arranged in shells. “Electron shells are labelled by giving each one a principal quantum number, n. For the first shell n = 1, for the second shell n = 2, etc. The higher the value of n, the further the shell is from the nucleus and so the greater is its energy. Each shell can hold more than one electron, but there is a limit” (Cronodon 2007), as shown in Table 16.

Table 16. Number of Electrons per Electron Shell. Adapted from Cronodon (2007).

Electron Shell	Principal Quantum Number	Maximum Number of Electrons
K	1	2
L	2	8
M	3	18
N	4	32

A shell is considered full when it contains the maximum number of electrons that it can store. The electrons within a given shell have a discrete amount of energy associated with it. Figure 27 provides a simple energy level diagram of the relationship between electron shells/principal quantum number and its associated energy.

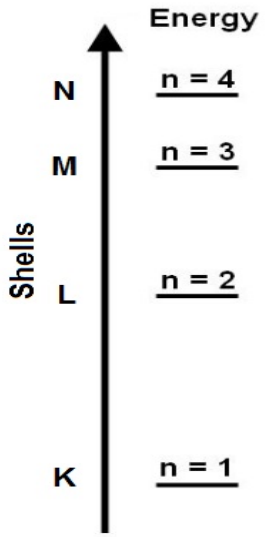

Figure 27. Energy Level Diagram of Electron Shells. Source: Cronodon (2007).

Electron shells are further split into sub-shells: s, p, d and f sub-shells. Each subshell can hold more than one electron, but there is a limit to each sub-shell (Cronodon 2007), as seen in Table 17.

Table 17. Electron Sub-shell and the Maximum Number of Electrons per Sub-shell. Source: Cronodon (2007).

Sub-shell	Maximum number of electrons
s	2
p	6
d	10
f	14

The sub-shells are housed within the electron shells and organized to their discrete engine levels, which adds more complexity to the energy level diagram. Figure 28 expands the energy level diagram to include each electron shells' sub-shells and their arrangement.

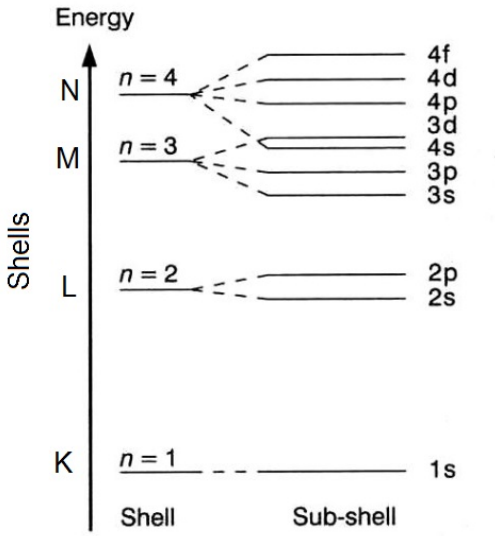

Figure 28. Energy Level Diagram of Electron Shells and Associated Sub-shells. Source: Cronodon (2007).

As noted on Cronodon.com, the K shell can only contain a maximum of two electrons. Those two electrons are housed in its only subshell, s. The L shell can only contain a maximum of eight electrons, two electrons in its s subshell, and six electrons in its p subshell (Cronodon 2007). The M shell can only contain a maximum of 18 electrons: two electrons in its s subshell, six electrons in its p subshell, and 10 electrons in its d subshell. And so forth (Cronodon 2007).

Within each subshell, electrons are further categorized by their orbital and direction of spin. Orbitals can only contain a maximum of two electrons. For example, the p subshell has three orbitals for its six allowable electrons: p_x, p_y, and p_z. The orbitals for the f and d subshells are more complex. Within each orbital, electrons are classified by their directions of spin, up or down (Cronodon 2007).

THIS PAGE INTENTIONALLY LEFT BLANK

LIST OF REFERENCES

Bryce, Douglas M. 1996. *Plastic Injection Molding—Manufacturing Process Fundamentals*. vol. 1. Dearborn, MI: Society of Manufacturing Engineers.

Buckleitner, Eric V., ed. 1995. *DuBois and Pribble's Plastics Mold Engineering Handbook*, 5th ed. New York: Chapman & Hall.

Chakrabarti, Amartya, Jun Lu, Jennifer C. Skrabutenas, Tao Xu, Zhili Xiao, John A. Maguire, and Narayan S. Hosmane. 2011. "Conversion of Carbon Dioxide to Few-layer Graphene." *Journal of Materials Chemistry*, 9491–9493.

Chen, Jian-Hao, Chaun Jang, Shudong Xiao, Masa Ishigami, and Michael S. Fuhrer. 2008. "Intrinsic and Extrinsic Performance Limits of Graphene Devices on SiO2." *Nature Nanotechnology* 5(8): 206–209.

Clayton, Paul R. 2006. *Introduction to Electromagnetic Compatibility*, 2nd ed. Hoboken, NJ: John Wiley & Sons.

Cronodon. 2007. "Introduction to Atoms." Last modified January 28. http://cronodon.com/Atomic/Atom_Intro.html.

Design Innovation. 2009. "Off-the-Shelf Enclosures –Part 4– Sheet Metal and Extruded Aluminum Pros and Cons." Last modified May 28. *Design Innovation Blog*. http://designinnovationblog.wordpress.com/tag/emi-shielding/.

Dieter, George E., and Linda C. Schmidt. 2013. *Engineering Design*, 5th ed. New York: McGraw Hill.

DoDD 5000.01, The Defense Acquisition System, Fed. Reg. (Nov. 20, 2007).

Dow Corning. 2014. *Sylgard 184 Silicone Elastomer*. Auburn MI: Dow Corning.

Fuchs, Jean-Noel, and Mark Oliver Goerbig. 2008. "Introduction to the Physical Properties of Graphene." Lecture presented at Laboratoire de Physique des Solides, Université Paris Sud, Orsay, France. https://www.equipes.lps.u-psud.fr/GOERBIG/CoursGraphene2008.pdf.

Graphenea. 2017. "Graphene Applications and Uses." Accessed June 27. https://www.graphenea.com/pages/graphene-uses-applications#.WVMDVlFOn3g.

Hanson, George W. 2008. "Dyadic Green's Functions and Guided Surface Waves for a Surface Conductivity Model of Graphene." *Journal of Applied Physics* 103(064302) (March 18). doi: 10.1063/1.2891452.

Hibino, H., S. Tanabe, S. Mizuno and H. Kageshima. 2012. “Growth and Electronic Transport Properties of Epitaxial Graphene on SiC.” *Journal of Physics D: Applied Physics* 45(154008) (March 29): 1–12. doi: 10.1088/0022-3727/45/15/154008.

Horton, Alex. 2017. “Army, Marine Corps Look to Lighten Load for Combat Troops.” *Stars and Stripes*, May 17. https://www.stripes.com/news/army-marine-corps-look-to-lighten-load-for-combat-troops-1.468816#.WUsjjVFOn3i.

Hurd, Colin M. 1972. *The Hall Effect in Metals and Alloys*. New York: Plenum Press.

Kittel, Charles. 2005. *Introduction to Solid State Physics*, 8th ed. Hoboken, NJ: John Wiley & Sons.

Langford, Gary O. 2012. *Systems Integration—Theory, Metrics, and Methods*. Boca Raton, FL: CRC Press.

Lee, Changgu, Xiaoding Wei, Jeffrey W. Kysar, and James Hone. 2008. “Measurement of the Elastic Properties and Intrinsic Strength of Monolayer Graphene.” *Science* 321(5887): 385–388.

Lovat, Giampiero. 2012. “Equivalent Circuit for Electromagnetic Interaction and Transmission through Graphene Sheets.” *IEEE Transactions on Electromagnetic Compatibility* 54(1) (February 17): 101–109.

Luxmi, Shu Nie, P. J. Fisher, R. M. Feenstra, Gong Gu, and Yugang Sun. 2009. “Temperature-dependence of Epitaxial Graphene Formation on SiC(0001).” *Journal of Electronic Material* 38(6): 718–724.

MatWeb. 2015. “MatWeb, Your Source for Materials Information.” Accessed August 21. http://www.matweb.com/.

———. 2017. “AISI 1018 Steel, Cold Drawn.” Accessed January 7. http://www.matweb.com/search/DataSheet.aspx?MatGUID=3a9cc570fbb24d119f08db22a53e2421.

Menges, Georg, and Paul Mohren. 1993. *How to Make Injection Molds*, 2nd ed. Munich: Hanser Publishers.

Mgrdichian, Laura. 2008. “A Smarter Way to Grow Graphene.” *PhysOrg*. http://phys.org/news129980833.html.

Moore, Donna. 2011. “Lightweight Electromagnetic Interference (EMI) Shielding System for Aircraft Avionics.” (Navy SBIR 2011.2—Topic N112-097). *Navy SBIR*. Last modified May 26. http://www.navysbir.com/n11_2/N112-097.htm.

Ott, Henry W. 2009. *Electromagnetic Compatibility Engineering*. Hoboken, NJ: John Wiley & Sons.

Pletikosić, I., M. Kralj, P. Pervan, R. Brako, J. Coraux, A. T. N'Diaye, C. Busse, and T. Michely. 2009. "Dirac Cones and Minigaps for Graphene on Ir (111)." *Physical Review Letters,* 102, 056808.

Rosato, Dominick V., Donald V. Rosato, and Marlene G. Rosato. 2000. *Injection Molding Handbook*, 3rd ed. Boston: Kluwer Academic Publishers.

Schroder, Dieter K. 2006. *Semiconductor Material and Device Characterization*, 3rd ed. Hoboken, NJ: John Wiley & Sons.

Stanley, William D., and Richard F. Harrington. 1994. *Lines and Fields in Electronic Technology*. Englewood Cliffs, NJ: Prentice Hall.

Sukang, Bae, Hyeongkeun Kim, Youngbin Lee, Xiangfan Xu, Jae-Sung Park, Yi Zheng, Jayakumar Balakrishnan, Tian Lei, Hye Ri Kim, Young Il Song, Young-Jin Kim, Kwang S. Kim, Barbaros Özyilmaz, Jong-Hyun Ahn, Byung Hee Hong, and Sumio Iijima. 2010. "Roll-to-roll Production of 30-inch Graphene Films for Transparent Electrodes." *Nature Nanotechnology* 5(8): 574–578.

Tong, Xingcun Colin. 2009. *Advanced Materials and Design for Electromagnetic Interference Shielding*. Boca Raton, FL: CRC Press.

Ulrich, Karl T., and Steven D. Eppinger. 2012. *Product Design and Development*, 5th ed. New York: McGraw-Hill Irwin.

Unarunotai, Sakulsuk, Yuya Murata, Cesar E. Chialvo, Hoon-sik Kim, Scott MacLaren, Nadya Mason, Ivan Petrov, and John A. Rogers. 2009. "Transfer of Graphene Layers Grown on SiC Wafers to Other Substrates and their Integration into Field Effect Transistors." *Applied Physic Letters*, 95, 202101.

University of Maryland. 2008. "Physicists Show Electrons Can Travel More Than 100 Times Faster in Graphene." Phys.org, March 24. https://phys.org/news/2008-03-physicists-electrons-faster-graphene-silicon.html.

U.S. Army Materiel Command. 2012. "Graphene." February 29. https://www.flickr.com/photos/armymaterielcommand/6795812766.

U.S. Department of Defense. 2015. *Requirements for the Control of Electromagnetic Interference Characteristics of Subsystems and Equipment*. MIL-STD-461G. Wright-Patterson AFB OH: U.S. Department of the Air Force.

Warner, Jamie H., Franziska Schaffel, Mark Rummeli, and Alicja Bachmatiuk. 2013. *Graphene: Fundamentals and Emergent Applications*, 1st ed. Saint Louis, MO: Elsevier.

Wikimedia. 2014. S.v. "File:Diamond and graphite.jpg." Last modified March 6. http://commons.wikimedia.org/wiki/File:Diamond_and_graphite.jpg.

———. 2016. S.v. "Injection Molding—Simplified Diagram. Illustration." Last modified November 26. https://commons.wikimedia.org/wiki/File:Injection_molding_diagram.svg#/media/File:Injection_molding_diagram.svg.

Zhengtang, Luo, Ye Lu, Daniel W. Singer, Matthew E. Berck, Luke A. Somers, Brett R. Goldsmith, and A. T. Charlie Johnson. 2011. "Effect of Substrate Roughness and Feedstock Concentration on Growth of Wafer-Scale Graphene at Atmospheric Pressure." *Chemistry of Materials* 23(6): 1441–1447.

INITIAL DISTRIBUTION LIST

1. Defense Technical Information Center
   Ft. Belvoir, Virginia

2. Dudley Knox Library
   Naval Postgraduate School
   Monterey, California